Mineralogy of Asteroids

M. J. Gaffey
University of North Dakota

E. A. Cloutis
University of Winnipeg

M. S. Kelley
NASA Johnson Space Center and Georgia Southern University

K. L. Reed
The Space Development Institute

The past decade has seen a significant expansion both in the interpretive methodologies used to extract mineralogical information from asteroid spectra and other remote-sensing data and in the number of asteroids for which mineralogical characterizations exist. Robust mineralogical characterizations now exist for more than 40 asteroids, an order a magnitude increase since *Asteroids II* was published. Such characterizations have allowed significant progress to be made in the identification of meteorite parent bodies. Although considerable progress has been made, most asteroid spectra have still only been analyzed by relatively ambiguous curve-matching techniques. Where appropriate and feasible, such data should be subjected to a quantitative analysis based on diagnostic mineralogical spectral features. The present paper reviews the recent advances in interpretive methodologies and outlines procedures for their application.

1. INTRODUCTION

In the beginning (ca 1801), asteroids were points of light in the sky. The primary measurements were positional, and the primary questions concerned the nature of their orbits. Despite some early attempts to determine their composition (e.g., *Watson,* 1941), the next major efforts in asteroid science occurred in the 1950s with the development of instrumental photometry, the measurement of asteroid light-curves, and investigations of rotational periods, body shapes, and pole orientations. The first true compositional investigations of asteroids began in 1970 with the study of asteroid 4 Vesta (*McCord et al.,* 1970) supported by spectral studies of minerals (*Burns,* 1970a,b; *Adams,* 1974,1975) and meteorites (*Salisbury et al.,* 1975; *Gaffey,* 1976). A parallel effort developed an asteroid taxonomy that was suggestive of — but not diagnostic of — composition (*Tholen,* 1984; *Tholen and Barucci,* 1989).

In the past decade, spacecraft flyby (951 Gaspra, 243 Ida, 253 Mathilde) and rendezvous (433 Eros) missions as well as high-resolution Hubble Space Telescope, radar, and adaptive-optics observations have removed asteroids from the "unresolved point source" class. This has allowed the surface morphology and shape of these bodies to be studied.

In a similar fashion, advances in meteorite science and remote-sensing capabilities have opened the early history of individual asteroids and their parent bodies to sophisticated investigation. The central questions of current asteroid studies focus on geologic issues related to the original compositions of asteroidal parent bodies and the chemical and thermal processes that altered and modified the original planetesimals. Based on the small size of the planetesimals and on meteorite chronologies, it is known that all significant chemical processes that affected these minor planets were essentially complete within the first 0.5% of solar-system history. Asteroids represent the sole surviving *in situ* population of early inner solar-system planetesimals, bodies from which the terrestrial planets subsequently accreted. Material in the terrestrial planets has undergone substantial modification since the time of planetary accretion. Hence, asteroids provide our only *in situ* record of conditions and processes in the inner (~1.8–3.5 AU) portions of the late solar nebula and earliest solar system.

The meteorites provide detailed temporal resolution of events in the late solar nebula and earliest solar system, but the spatial context for that information is poorly constrained. Asteroid compositional studies, by elucidating relationships between individual asteroids and particular meteorite types, provide a spatial context for the detailed meteoritic data. Moreover, asteroid studies can identify types of materials not sampled in the terrestrial meteorite collections. The major goal of current asteroid investigations is to better understand the conditions and processes that prevailed in the late solar nebula and early solar system.

It is no longer possible to view asteroid studies as isolated from meteoritic and geologic constraints. One major corollary of this reality is that interpretations of asteroid compositions must be consistent with the nature of meteorites and with the geologic processes that produced or were active within the parent bodies. If different techniques give conflicting answers for an individual body, at best only one can be correct. And if one must choose between competing interpretations, one should select the most geologically and meteoritically plausible option. If one invokes an esoteric asteroid assemblage, the onus is on the investigator to justify it geologically. (For example, if one were to interpret a 50-km asteroid as being composed of kaolinite, one must be able to describe plausible geologic or meteorite parent body conditions for producing a 50-km mass of kaolinite!) Interpretations without geologic or meteoritic support must be considered as suspect until plausible geologic formation processes can be defined. A solid grounding in meteoritics and geology should now be considered as a prerequisite to the analysis of asteroid compositions.

The meteorites also constrain how we think about the asteroids. It is now clearly evident that the meteorite collection is an incomplete and biased sample of its asteroidal source region(s). For example, at least half of the mineral assemblages that geochemical considerations indicate should be formed with the known meteorite types are not represented in our collections. There are >55 types of asteroid-core material present as magmatic iron meteorites in our collections. The corresponding mantle and crust lithologies are essentially absent from these collections. The meteorites, nevertheless, provide strong constraints on the sampled portion of the asteroid belt. *Keil* (2000) has shown that ~135 individual meteorite parent bodies have contributed samples to our meteorite collections. Of these ~135 parent bodies, 80% have experienced strong heating that produced partial to complete melting. Thus, in the meteorite source regions (presumably primarily the inner belt), igneous asteroids are the rule rather than the exception. *Keil* (2000) also notes that the 20% of meteorite parent bodies that did not experience at least partial melting did experience heating to some degree.

Thus in thinking about at least the inner asteroid belt, one should consider that a large portion of the bodies we see probably either experienced strong heating or are fragments of parent bodies that experienced strong heating. This is the reverse of an older view (e.g., *Anders,* 1978) that most meteorite parent bodies, and by inference asteroids, are primarily primitive (i.e., chondritic) bodies.

Several of the major scientific issues that could benefit most significantly from sophisticated mineralogical characterizations of asteroids to be properly addressed include (1) constraining the conditions, chemical properties, and processes in the inner solar nebula as it evolved into the solar system; (2) independently confirming the dynamical pathways and mechanisms that deliver asteroidal bodies and their meteoritic fragments into Earth-crossing orbits; (3) characterizing additional types of materials present in the asteroid belt but not sampled in the meteorite collections; and (4) defining the chemical and thermal evolution of the planetesimals prior to accretion into the terrestrial planets.

2. BEFORE THE ANALYSIS CAN PROCEED

Mineralogical characterizations of asteroids — often somewhat inaccurately termed "compositional" characterizations — rely primarily on the identification and quantitative analysis of mineralogically diagnostic features in the spectrum of a target body. However, before such features can be identified and used for mineralogical characterizations, the spectrum must be properly reduced and calibrated. Inadequate reduction and calibration can introduce spurious features into the spectrum and/or suppress or significantly distort real features in the spectrum.

2.1. Atmospheric Extinction Corrections

Spectra begin their existence as measurements of photon flux vs. wavelength. These measurements may involve discrete filters, variable filters where bandpass is a function of position, interferometers, or dispersion of the spectrum by prism or grating. These raw flux measurements are converted to reflectance or emission spectra by ratioing the flux measurements at each wavelength for the target object (e.g., an asteroid) to a reference standard measured with the same system. For reflectance spectra this can be expressed schematically as

$$\text{Reflectance}_\lambda\ (\text{object}) = \text{Flux}_\lambda\ (\text{object})/\text{Flux}_\lambda\ (\text{standard}) \quad (1a)$$

This ratioing procedure removes the wavelength-dependent instrumental sensitivity function. If the standard object (typically a star) has a Sun-like wavelength-dependent flux distribution, the resulting ratio is a true relative reflectance spectrum (i.e., relative fraction of light reflected as a function of wavelength). If the standard does not have a Sun-like flux distribution, the object:standard ratio needs to be corrected at each wavelength for this difference. This is shown schematically by

$$\text{Reflectance}_\lambda\ (\text{obj}) = \text{Flux}_\lambda\ (\text{obj})/\text{Flux}_\lambda\ (\text{star}) \times \text{Flux}_\lambda\ (\text{star})/\text{Flux}_\lambda\ (\text{Sun}) \quad (1b)$$

For groundbased telescopic observations, this conceptually simple procedure is complicated by the transmission function of the terrestrial atmosphere. Equations (1a) and (1b) are strictly true only if both the object and the standard are observed simultaneously through the same atmospheric path. This is almost never the case. There are several methods of overcoming this problem. The simplest and most commonly used approach is to divide the object flux spectrum by a standard star flux spectrum, where the standard star observation is chosen to have an airmass (atmospheric path length) similar to the object observation and to have been

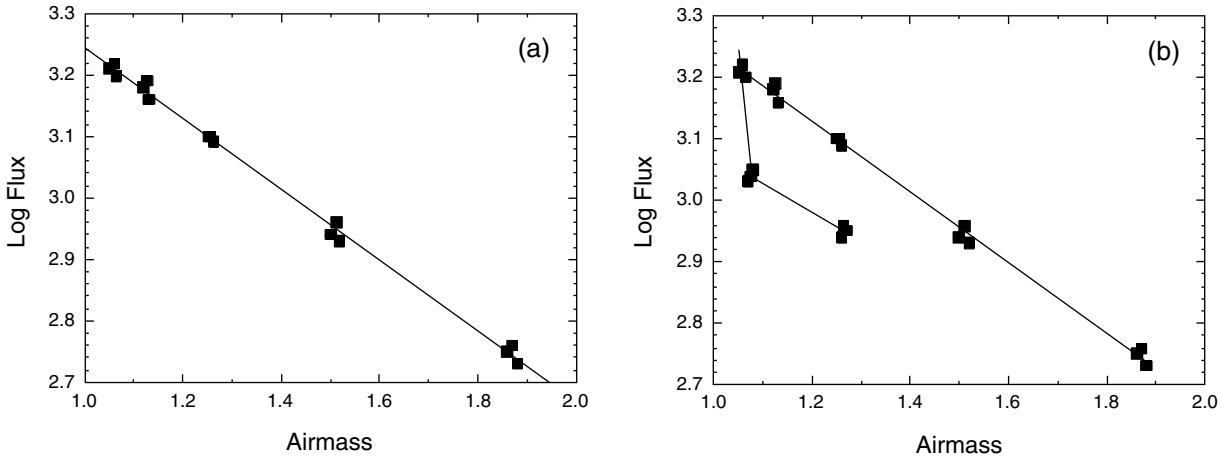

Fig. 1. **(a)** A schematic extinction curve for a particular wavelength computed from the measured fluxes at that wavelength for a standard star observed over a range of airmasses during a single night with stable and uniform atmospheric transmission. The absorption is assumed to follow a Beer-Lambert law, where the log of the flux is linear with the airmass. Airmass is calculated as the secant of the angle away from the zenith. **(b)** A schematic extinction curve where there is either an east-west asymmetry in the sky or the atmospheric transmission changed about the time the standard star crossed the meridian.

observed within a short time interval of the object observation. There are no strict criteria on what constitutes "similar" and "short." One can also extrapolate the standard star fluxes to the airmass of the object observation using standard extinction coefficients (atmospheric flux attenuation per unit airmass as a function of wavelength) for the particular observatory. Operationally, a ratio is acceptable when the atmospheric absorption features are "minimized." This may involve the division of an individual observation by a number of standard star observations until an acceptable ratio is generated. Clearly this is most easily accomplished for spectral regions where the extinction coefficient is small (i.e., no strong atmospheric absorptions), but still involves a significant subjective selection of "best."

A more rigorous means of removing the effects of differential atmospheric transmission involves computation of the extinction coefficients for each night or portion of a night. This is shown schematically in Fig. 1a. The slope and intercept of the linear least-squares fit can be used to compute the effective flux of that standard star at any airmass in the appropriate interval. The set of slopes and intercepts for all wavelengths of the observations is termed a "starpack." The slopes in a starpack should mimic the atmospheric transmission as a function of wavelength. Figure 1a shows the fit to standard flux measurements at a particular wavelength when the atmospheric transmission is stable over time and symmetric about the zenith. More typically, neither of these conditions is met, and the result is shown in Fig. 1b. For example, at Mauna Kea Observatory, there is commonly an upwind/downwind asymmetry in the extinction. This is due to the presence of a very thin (usually imperceptible to the eye) orographic haze formed over the peak and extending some distance downwind. The pattern shown in Fig. 1b is the result of extra absorption in the eastern sky (downwind) as the object rises toward the meridian. When the object passes the western edge of the cloud, the flux rises. As the object moves westward to higher airmass, the regular extinction slope is seen. As would be expected, the effect is most pronounced at the wavelengths of the atmospheric water features.

2.2. Special Instrumental Considerations

Additionally, most instrumental systems used for asteroidal observations have their own special "quirks" that can affect final reflectance spectra. Since asteroid spectral studies often push the capabilities of telescopic instruments, it is important to be sensitive to the presence of such special data-reduction requirements, which may be of little or no significance to classical astronomers. Although space limitations do not permit a full discussion of such quirks in the variety of instruments that have been used to obtain asteroid spectra, previous examples include the beam inequality and coincidence counting effects in the two-beam photometer system (*Chapman and Gaffey,* 1979), lightcurve-induced spectral slopes in CVF and filter-photometer systems (e.g., *Gaffey et al.,* 1992; *Gaffey,* 1997), and channel shifts in CCD and other array detectors as evidenced by the mismatch of the narrow atmospheric O_2 absorption line at 0.76 μm in unedited spectra (e.g., *Xu et al.,* 1995; *Vilas and Smith,* 1985; *Vilas and McFadden,* 1992).

The recent advent of moderate-resolution ($\lambda/\Delta\lambda \sim 100$–500) asteroid observations with NIR array detectors has produced a particularly keen need to detect and compensate for potential subtle instrumental artifacts in the resulting spectra. At these resolutions, small shifts in the placement of the dispersed spectrum onto the detector (due to unavoidable instrument flexure) produce significant artifacts in the re-

flectance spectrum in regions where the measured flux is changing rapidly with wavelength. This is shown in Fig. 2.

Even a small shift in the location of the spectrum on the detector (1 channel or ~1/500 of the length of the dispersed spectrum) produces significant structure in the resulting ratio as shown by Fig. 2b. The effect is most pronounced where the spectral flux changes most rapidly from channel to channel, such as the short wavelength edge of the 1.4-μm atmospheric water-vapor band. In that region, a distinct spike is observed, which is negative (below the background curve) when the channel shift of the "numerator" spectrum is positive relative to the "denominator" spectrum and positive (above the background curve) when the channel shift is negative. If spikes at a few channels around the steepest portions of the flux curves were the sole effect, those points could simply be deleted with little loss of data.

However, examination of Fig. 2b shows that the effect of such a shift is much more pernicious. For example, consider the region around 1.4 μm, where the ratio is ~10% high. In an asteroid:star ratio (reflectance spectrum), the negative spike near 1.34 μm could be readily detected and deleted. However, the ratio would still overestimate the reflectance by ~10%, decreasing to 0% between ~1.36 and 1.5 μm. Since this is a region where the plagioclase feldspar feature is observed in eucrite meteorites and Vesta-type spectra, the presence of this effect would distort the feldspar feature, either increasing or decreasing its apparent intensity depending on the relative direction of the channel shift.

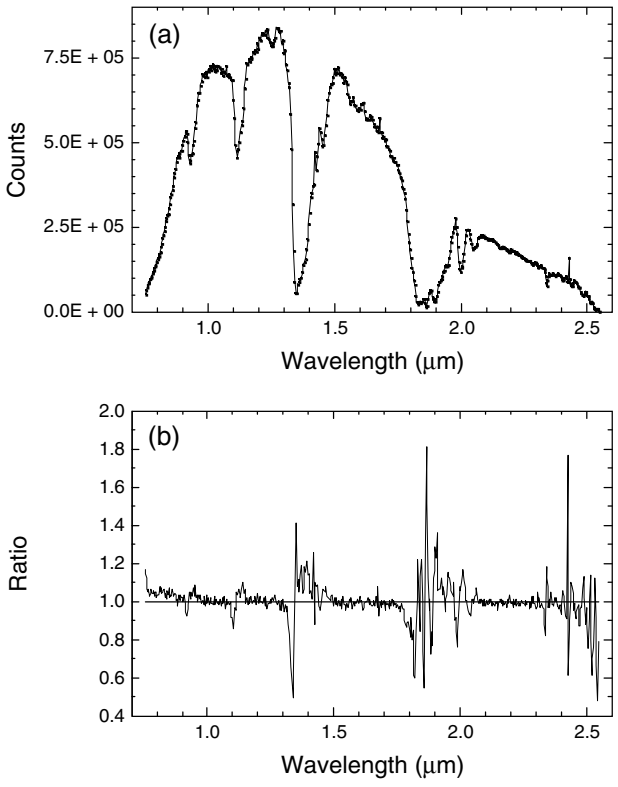

Fig. 2. **(a)** Spectral flux distribution (instrumental counts vs. wavelength) for standard star BS5996 observed with a NIR-array spectrometer (the SpeX Instrument operating in low resolution or asteroid mode at the NASA Infrared Telescope Facility at Mauna Kea Observatory). **(b)** Ratio of flux for this observation offset by +1 channel (~1/500 the length of the spectrum on the array detector) relative to the original data. Without the channel offset the ratio would lie on the heavy line at 1.0.

From the point of view of characterizing asteroid mineralogy, the effect is most severe on Band II, the ~2-μm pyroxene-absorption feature present in varying intensities in the spectra of most chondrites, basaltic achondrites, ureilites, SNCs, lunar samples, and S-, V-, and R-type asteroids. This feature is generally centered between 1.8 and 2.1 μm. Again referring to Fig. 2b, one effect of a +1 channel shift is the introduction of a high-frequency noise component, degrading the quality of the ratio spectrum between 1.8 and 2.1 μm. But more importantly, the ratio curve will be up to 15% low between 1.75 and 1.80 μm and up to 15% high between 1.9 and 2.02 μm. This would have the effect of shifting the effective band center toward a shorter wavelength, resulting in an erroneous determination of pyroxene composition. The opposite effect would be observed if the channel shift was in the opposite direction (i.e., –1 channel). The magnitude of the change in the apparent spectrum is generally comparable to — and often greater than — the intensity of Band II in S-type spectra. The actual magnitude of these effects will depend on the magnitude of the channel shift. Unless detected and corrected, this effect has the potential to significantly distort the position, shape, and intensity of the absorption feature (and hence, the interpreted mineralogy).

3. INTERPRETIVE METHODOLOGIES FOR THE MINERALOGICAL ANALYSIS OF ASTEROID SPECTRA

3.1. Taxonomy

Taxonomy is the classification of a group of subjects (objects, phenomena, organisms, etc.) into classes based on shared measured properties. The utility of any taxonomy is a function of the relevance of the properties employed in the classification. In the case of the asteroid taxonomic classes, the parameters are observational (e.g., spectral slope, color, albedo, etc.) but in most cases are not particularly diagnostic of either mineralogy or composition. It is generally safe to assume that objects in different taxonomic classes are physically or compositionally different from each other, although the nature of the difference is generally not well constrained. However, the converse is not true. It is not safe to assume that members of a taxonomic class have similar compositions, mineralogies, or genetic histories.

The reliance on asteroid taxonomy, while useful for suggesting both similarities and differences between asteroids, is seductive and can actually impede geological interpretation of the asteroid belt. Assuming that such classifications imply some mineralogical or petrogenetic similarities among all (or most) members of a class may not be

warranted and can be counterproductive (e.g., *Gaffey et al.,* 1993b). For example, the early debate over the S-asteroid class was largely focused on whether this group consisted of differentiated or primitive objects. Recent interpretations of individual S-asteroid spectra indicate that this class includes both differentiated and primitive members (*Gaffey et al.,* 1993a, and references therein; *Gaffey and Gilbert,* 1998; *Kelley and Gaffey,* 2000). The S class has now been subdivided into a number of mineralogical subclasses, which may be further subdivided as new data and interpretations are generated. We have seen a similar expansion in the overall number of asteroid classes over the years as the quantity and quality of observational data have improved. At some point the knowledge of individual asteroids becomes sufficiently detailed that their class becomes largely redundant, just as the classification "mammal" becomes largely redundant when one is investigating the relationships between different members of the "cat" family.

3.2. Curve Matching

For many years, analysis of asteroid reflectance spectra relied on a comparison to laboratory reflectance spectra of meteorites (e.g., *Chapman and Salisbury,* 1973; *Chapman,* 1976). This approach provided many important insights into plausible surface mineralogies for many asteroids, but had a number of limitations and could lead to incorrect interpretations or an unnecessarily restricted range of possible mineralogies. Limitations of this approach include (1) the fact that it generally cannot provide robust insights into surface mineralogies of asteroids that have no spectrally characterized meteorite analogs, (2) the lack of spectral reflectance data for terrestrially unweathered samples of many meteorite classes, and (3) the spectral variations associated with changes in grain size, viewing geometry, and temperature (e.g., *Adams and Filice,* 1967; *Egan et al.,* 1973; *Singer and Roush,* 1985; *Gradie and Veverka,* 1986; *Lucey et al.,* 1998). Moreover, extrinsic effects such as space weathering can modify the spectral shape and obscure potential genetic links to meteorites. Nevertheless, curve matching is useful for identifying the possible reasons asteroid spectra differ from possible meteorite analog spectra.

A similar spectral shape between an asteroid and a comparison sample (e.g., a meteorite or simulant) may suggest that they are composed of similar materials, but alternative interpretations are often possible. Initially, there is the issue of incompleteness of the comparison sample set. Curve matching will select the closest match to the asteroid spectrum from among the sample set. However, if — as is almost always the case — the sample set is not exhaustive, the match may not be meaningful.

The second issue with curve matching is exactly what is meant by "similar." For example, a numerical algorithm can be used to estimate the mean deviation between an asteroid spectrum and a suite of comparison spectra in order to select the sample or mixing model that most closely matches the asteroid. This has been done by a number of investigators (e.g., *Hiroi et al.,* 1993; *Clark,* 1995). However, the match is generally to the entire available spectral curve. Such a "full-spectrum" match does not address the issue of which portions of the spectrum are most significant. For example, the position and shape of the centers of the absorption features must be matched very closely to have any confidence in the result. By contrast, even very poor matches to the spectral curve outside the absorption features may be of little or no significance. Thus "curve matching" can only provide a reasonably credible result when a wavelength-dependent weighting function is applied to account for the relative importance of the match in different spectral intervals. To date, no such wavelength-weighted matching procedure has been used, and thus all curve matching results should be viewed with at least some skepticism.

3.3. Mineralogical Analysis of Spectra

Mineralogical characterizations of asteroids — and investigations of possible genetic linkages to meteorites — involve analysis of spectral parameters that are diagnostic of the presence and composition of particular mineral species. Not all minerals — nor even all meteoritic minerals — have diagnostic absorption features in the visible and NIR (VNIR) spectral regions where most asteroid data have been obtained. Fortunately, a number of the most abundant and important meteoritic minerals do exhibit such diagnostic features. The most important set are crystal field absorptions arising from the presence of transition metal ions [most commonly bivalent iron/Fe^{2+}/Fe(II)] located in specific crystallographic sites in mafic (Mg- and Fe-bearing) silicate minerals. Mafic minerals (e.g., olivine, pyroxene, certain Fe-phyllosilicates, etc.) are the most abundant phases in all chondrites and in most achondrites. They are also present as the major silicate phases in stony irons and as inclusions in a significant number of iron-meteorite types. A mineral is a particular composition (or range of compositions in the case of a solid-solution series) formed into a particular crystallographic structure. The wavelength position, width, and intensity of these crystal-field absorptions are controlled by structure and composition that are directly related to the fundamental definition of a mineral. The quantum-mechanics-based theory behind these features is summarized by *Burns* (1970a,b, 1993). *Adams* (1974, 1975), *Salisbury et al.* (1975), *Gaffey* (1976), *King and Ridley* (1987), *Gaffey et al.* (1989), *Cloutis and Gaffey* (1991a,b), and *Calvin and King* (1997) show examples of the reflectance spectra of meteorites and the minerals of which they are made.

3.3.1. Mafic mineral compositions. The relationship between diagnostic spectral parameters (especially absorption-band center positions) for reflectance spectra of a number of mafic minerals, particularly pyroxene and olivine, was first outlined by *Adams* (1974, 1975) and revisited by *King and Ridley* (1987) and *Cloutis and Gaffey* (1991a). All these spectral measurements were made at room temperature. In equation form, the relationships between ab-

sorption-band center and pyroxene composition (molar Ca content [Wo] and molar-Fe content [Fs]) shown in those papers can be expressed as

$$\text{Wo } (\pm 3) = 347.9 \times \text{BI Center } (\mu\text{m}) - 313.6 \quad (\text{Fs} < 10;\ \text{Wo}_{\sim 5-35} \text{ excluded}) \tag{2a}$$

$$\text{Wo } (\pm 3) = 456.2 \times \text{BI Center } (\mu\text{m}) - 416.9 \quad (\text{Fs} = 10\text{–}25;\ \text{Wo}_{\sim 10-25} \text{ excluded}) \tag{2b}$$

$$\text{Wo } (\pm 4) = 418.9 \times \text{BI Center } (\mu\text{m}) - 380.9 \quad (\text{Fs} = 25\text{–}50) \tag{2c}$$

$$\text{Fs } (\pm 5) = 268.2 \times \text{BII Center } (\mu\text{m}) - 483.7 \quad (\text{Wo} < 11) \tag{3a}$$

$$\text{Fs } (\pm 5) = 57.5 \times \text{BII Center } (\mu\text{m}) - 72.7 \quad (\text{Wo} = 11\text{–}30,\ \text{Fs}_{<25} \text{ excluded}) \tag{3b}$$

$$\text{Fs } (\pm 4) = -12.9 \times \text{BII Center } (\mu\text{m}) + 45.9 \quad (\text{Wo} = 30\text{–}45) \tag{3c}$$

$$\text{Fs } (\pm 4) = -118.0 \times \text{BII Center } (\mu\text{m}) + 278.5 \quad (\text{Wo} > 45) \tag{3d}$$

Note that the "excluded" ranges in the Wo calibrations (equations (2a) and (2b)) and the Fs calibration (equation (3b)) represent compositions not present among natural minerals (*Deer et al.,* 1963, p. 5).

No single equation is applicable to the full range of pyroxene compositions. The values in parentheses after each equation indicate the range of compositions to which that equation applies. The uncertainty indicated for each determination is the mean of the differences (rounded up to the next whole number) between the predicted and measured compositions among the set of samples used to establish each calibration.

Since neither the Ca nor Fe content is known initially, these equations are used in an iterative fashion to derive the pyroxene composition. The following example illustrates this process. The Band I and Band II positions of a pyroxene-dominated asteroid spectrum are 0.937 and 1.914 μm respectively. The dominance of pyroxene can be established by a high band-area ratio (see below) or an unbroadened 1-μm absorption feature. From equation (2a), the 0.937-μm Band I center corresponds to Wo_{12}. This value indicates that among the equation (3) options, equation (3b) (appropriate for $Wo_{11–30}$) should be used. Plugging the Band II center wavelength into equation (3b) gives a value of 37 (Fs_{37}). However, the initial Wo determination was made with equation (2a), which is appropriate only for $Fs_{<10}$. Based on the Fs determination, equation (2c) should be used and gives a value of 11.6 (Wo_{12}). This is consistent with the use of equation (3b), so the process has converged. The possible alternate computations are:

Equation (3a) and Band II → Fs_{29} ⇒
Equation (2c) and Band I → Wo_{12} ⇒
Equation (3b) and Band II → Fs_{37}

Equation (3b) and Band II → Fs_{37} ⇒
Equation (2c) and Band I → Wo_{12}

Equation (3c) and Band II → Fs_{21} ⇒
Equation (2b) and Band I → Wo_{11} ⇒
Equation (3b) and Band II → Fs_{37}

Equation (3c) and Band II → Fs_{21} ⇒
Equation (2b) and Band I → Wo_{11} ⇒
Equation (3a) and Band II → Fs_{30}

Equation (3d) and Band II → Fs_{52} ⇒
Equation (2c) and Band I → Wo_{12} ⇒
Equation (3b) and Band II → Fs_{37}

Equation (2b) and Band I → Wo_{11} ⇒
Equation (3a) and Band II → Fs_{30} ⇒
Equation (2c) and Band I → Wo_{12}

Equation (2b) and Band I → Wo_{11} ⇒
Equation (3b) and Band II → Fs_{37}

Equation (2c) and Band I → Wo_{12} ⇒
Equation (3b) and Band II → Fs_{37}

The results are relatively insensitive to the pathway chosen. All converge on $Wo_{11–12}$ and Fs_{37} or Fs_{30}. The Wo content near 11 mol% produces the ambiguity in the Fs content, since it allows selection of either equation (3a) or (3b) to determine the Fe content.

The relationship between absorption-band position and olivine composition was explored by *King and Ridley* (1987). Unfortunately, the band shift with composition in olivine is small and band position provides a relatively poor constraint on olivine composition.

3.3.2. Mafic mineral abundances. *Cloutis et al.* (1986) developed a calibration between abundance in olivine-orthopyroxene (Ol-Opx) mixtures and the ratio of areas for the 1- and 2-μm absorption bands (Band II/Band I area; Band Area Ratio; BAR). Figure 3 shows a typical spectrum with the individual band areas indicated. (All these spectral measurements were made at room temperature.) For the interval of 10–90% orthopyroxene, this relationship can be expressed as:

$$\text{Opx}/(\text{Opx} + \text{Ol}) = (0.417 \times \text{BAR}) + 0.052 \tag{4}$$

It should be emphasized that this relationship applies directly only to olivine-orthopyroxene mixtures. An increasing error will be introduced by the presence an increasing clinopyroxene component in the mixture.

The Band I center position of an olivine-pyroxene mixture is a function of both the pyroxene composition (equations (2) and (3) above) and the olivine-pyroxene abundance ratio. Using the Band I center and BAR calibrations of *Cloutis et al.* (1986), a correction factor can be applied to the measured Band I center to remove the effect of olivine. Figure 4 shows the displacement in the Band I center as a function of BAR. When this correction factor is applied to

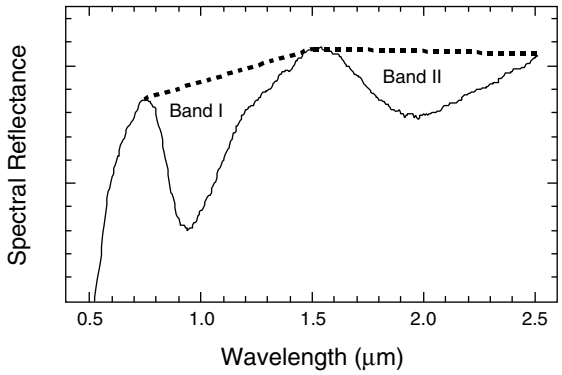

Fig. 3. The spectral reflectance curve of an olivine-pyroxene dominated meteorite sample (average LL3 chondrite). Band I and Band II are indicated. The band areas are the areas between the spectral curve and linear continua (shown as dashed lines) fitted tangent to the spectral curve at the edge of the absorption feature. The band area ratio (BAR) is the ratio of the area of Band II to that of Band I (BII/BI). Band centers are calculated by dividing out the linear continuum (to remove the effects of spectral slope) and fitting a polynomial function to the wavelength interval around the minimum in the ratioed curve.

the Band I center for olivine-orthopyroxene mixtures, the resulting Band I (corrected) and Band II values should plot along the pyroxene trend line shown by *Adams* (1975) and *Cloutis and Gaffey* (1991a). This provides a test of the validity of derived band positions. It also allows a "first-cut" determination of the calcic (Wo) content of the pyroxene.

The weak plagioclase feature near 1.25 μm in plagioclase-pyroxene mixtures (e.g., the eucrite members of the HED meteorite group) can be used to determine the plagioclase-pyroxene abundance ratio. *Gaffey et al.* (1989) describes the preliminary quantative calibration outlined by *McFadden and Gaffey* (1978).

3.3.3. One or two pyroxenes? Depending on their petrogenesis, anhydrous mafic rock assemblages (i.e., those dominated by Fe- and Mg-bearing silicates, such as olivine and pyroxene) commonly contain either a pyroxene of a single composition or two coexisting pyroxene compositions related by an equilibration constant dependent upon the geologic processes that formed the assemblage. The calibrations of 1- and 2-μm band positions to pyroxene composition [*Adams* (1974); *Cloutis and Gaffey* (1991a); equations (2) and (3)] work well for spectra from samples that contains a single pyroxene. However, the calibrations break down when a significant amount of a second pyroxene component is present.

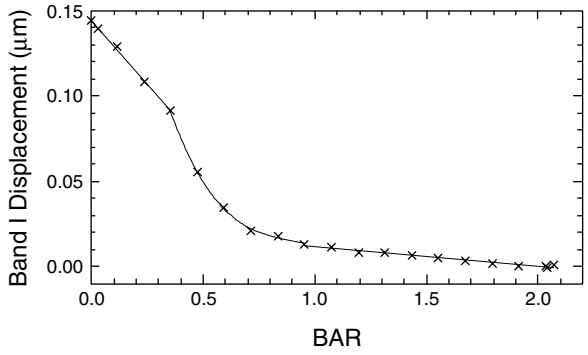

Fig. 4. The displacement in the Band I center in olivine-orthopyroxene mixtures relative to the Band I center for the pyroxene phase as a function of the band area ratio (BAR). BAR is inversely proportional to olivine abundance.

TABLE 1. Comparison of predicted and observed Band II centers for ordinary chondrites.

	H Chondrites	L Chondrites	LL Chondrites
Pyroxene composition*	$Fs_{17.2}$	$Fs_{21.3}$	$Fs_{24.1}$
Expected Band II center	1.868 μm	1.883 μm	1.893 μm
Observed Band II center	1.931 μm	1.944 μm	1.976 μm
Difference (actual — expected)	+0.063 μm	+0.061 μm	+0.083 μm

**Gomes and Keil* (1980).

An example of this discrepancy is evident when the above calibrations are applied to the Band II positions for the ordinary chondrites. These positions (e.g., *Gaffey,* 1976) are longward of the expected wavelengths based on the orthopyroxene compositions commonly cited for ordinary chondrites. This is shown on Table 1.

This discrepancy is not caused by the olivine component, since the spectra of olivine:orthopyroxene mixtures do not show this shift. In ordinary chondrites, low-Ca orthopyroxene is the dominant pyroxene phase, but there is a small but spectrally significant high-Ca pyroxene (diopside/augite) component. In the older meteorite literature, the high-Ca pyroxene component was not generally distinguished (or distinguishable) because of its small grain size and/or its presence only as very fine exsolution lamellae in orthopyroxene. As a result, often only the dominant orthopyroxene component was reported. *Brearley and Jones* (1998, p. 3-231) note that high-Ca pyroxene (augite) is the third most abundant silicate mineral component in the matrix of unequilibrated ordinary chondrites. *McSween et al.* (1991) include high-Ca pyroxene (diopside) in their normative calculations of ordinary chondrite mineralogy. Their calculations indicate that high-Ca pyroxene accounts for approximately 12%, 17%, and 19% of the pyroxene in average H-, L-, and LL-chondrites, respectively.

The high-Ca component in these chondrites has a composition of ~$Fs_{10}Wo_{45}$. The Band I and II positions for such a pyroxene are approximately 1.03 μm and 2.30 μm. On Fig. 5, the *Adams* (1974) and *Cloutis and Gaffey* (1991a) band positions are plotted for opx and cpx (small open symbols); the average band positions for H, L, and LL chondrites (large solid symbols); the expected band positions for the low-Ca (opx) in these chondrites based on the calibrations discussed above (large open symbols); the band position for the high-Ca pyroxene in these meteorites (large square with enclosed X); and the Band I position corrected

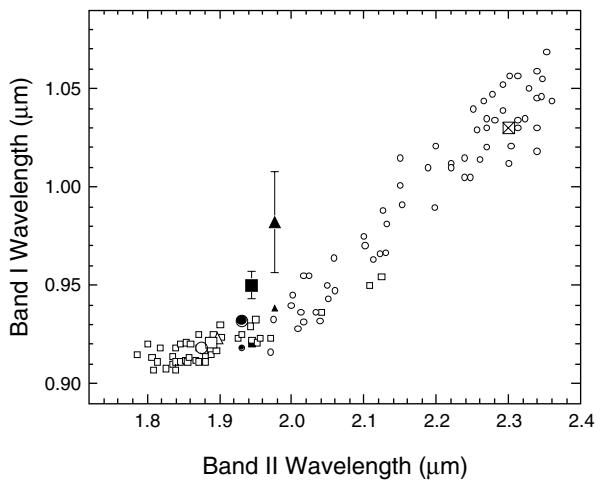

Fig. 5. Plot of Band I center vs. Band II center for low- and high-Ca pyroxenes from *Adams* (1974) and *Cloutis and Gaffey* (1991a) (small open squares and circles respectively). The average measured band positions for H, L, and LL chondrites (large solid symbols: circle, square, and triangle respectively) are compared to the "olivine corrected" band positions (small solid symbols) and the positions of the low-Ca pyroxene components (large open symbols) for these chondrites. The position of the high-Ca pyroxene component of these chondrites is plotted as square with an inscribed "X."

for olivine using the relationship shown in Fig. 3 (small solid symbols).

The ordinary chondrites are longward of their expected wavelengths based on their commonly cited pyroxene compositions, as shown in Table 1. The effect of the second (high-Ca) pyroxene (~$Fs_{10}Wo_{45}$) on the Band II position in ordinary chondrites appears to be an almost-linear function of the relative abundance of the two pyroxenes. The comparison between the fraction of the pyroxene that is high-Ca from average normative mineralogy (*McSween et al.,* 1991) and the abundance calculated from the Band II position assuming a linear relationship is summarized in Table 2. The agreement is sufficiently good to support the assumption that the Band II position is approximately a linear function of the abundances of the low-Ca and high-Ca pyroxene components in such assemblages.

Sunshine et al. (2002) have raised the intriguing possibility of S-type asteroids with silicates consisting solely of low-Ca orthopyroxene and high-Ca clinopyroxene. They identified two such asteroids (17 Thetis and 847 Agnia) that have BAR values normally indicating a substantial olivine component. Obviously the calibration (equation (4)) for pyroxene abundance in an olivine-orthopyroxene assemblage would be inappropriate for such assemblages. Therefore it is important to establish the applicability of this calibration before simply applying it to an S asteroid. Fortunately, there is a procedure for doing so.

TABLE 2. Comparison of normative and spectrally derived high-Ca pyroxene abundance.

	H Chondrites	L Chondrites	LL Chondrites
High-Ca/total pyroxene (normative)	12%	17%	19%
High-Ca/total pyroxene (spectra)	13%	14%	20%

Figure 4 shows the displacement off of the pyroxene trend (Fig. 5) as a function of the BAR value in olivine-orthopyroxene mixtures. If the displacement derived from the BAR value is subtracted from the Band I position for an olivine-orthopyroxene assemblage, the resulting point will fall on the pyroxene trend. The same procedure for a mixture of Ca-poor orthopyroxene and calcic clinopyroxene will result in a point below the pyroxene trend line. Thus the band center positions and the BAR value for an S-type spectrum can be used to establish whether or not equation (4) is applicable to that spectrum.

3.3.4. "Featureless" spectra. Analysis of asteroid spectra will not necessarily provide a complete inventory of the minerals that reside on the surface. Spectral analysis is only capable of detecting the presence of spectrally dominant minerals, i.e., those that possess unique or distinguishable spectral properties. These minerals may or may not be the most abundant. The minerals that are spectrally dominant will depend on the other phases that may be present. As an example, opaque materials such as macromolecular organics and magnetite, present in carbonaceous chondrites at the few weight percent level, tend to dominate the spectral signature of these meteorites, in spite of the fact that other minerals, such as olivine and layer lattice silicates are much more abundant (e.g., *Cloutis,* 1996; *Cloutis and Gaffey,* 1994). This spectral dominance is attributable to the fact that these opaque components are fine-grained, dispersed throughout the meteorites, and very effective absorbers of incident light (Fig. 6a). As a result, most carbonaceous chondrite VNIR spectra exhibit low reflectance and very subdued or undetectable absorption bands, even when their predominant olivine or layer lattice silicate constituents exhibit strong features (e.g., *Calvin and King,* 1997). *Clark and Lucey* (1984) demonstrated a similar suppression of strong water-ice features with the addition of a very small carbon black component to the ice.

Meteoritic metal, whether present as part of the original lithology or arising from reduction of ferrous Fe by a reducing agent (e.g., C) at elevated temperatures (e.g., *Walker and Grove,* 1993) or by the impact melting of minerals (*Hapke,* 2001) is an example of a material with no well-defined absorption features in the visible and NIR spectral regions. The presence of this material in many asteroid reflectance spectra is inferred by the way it modifies the spectra of mafic silicates with which it is associated. Figure 6b shows the reflectance spectra of pure olivine, meteoritic metal, and a 50:50 intimate mixture of this olivine and meteoritic metal. The spectrum of the mixture is very similar to that of the metal, particularly in terms of overall slope, which increases toward longer wavelengths. This spectral shape, commonly referred to as red-sloped, is characteristic of many S-class asteroid spectra (*Gaffey et al.,* 1993a,b). This

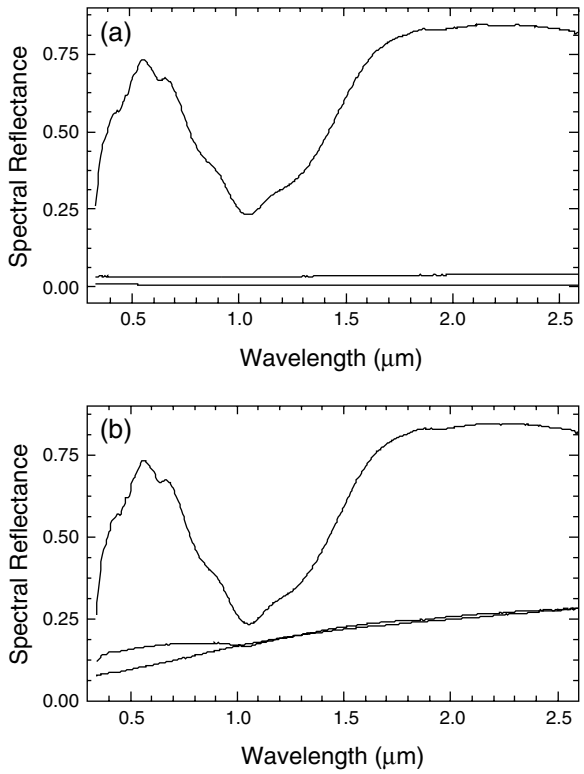

Fig. 6. **(a)** Reflectance spectra of 45–90-μm grain size olivine (upper curve), <0.021-μm size C lampblack (lower curve), and an intimate mixture of 98 wt% olivine and 2 wt% C lampblack (middle curve). Note: Bottom axis is –0.05. **(b)** Reflectance spectra of 45–90-μm grain size olivine (upper curve), 45–90-μm size metal from the Odessa iron meteorite (lower curve at 0.5 μm), and an intimate mixture of 50 wt% olivine and 50 wt% metal (middle curve at 0.5 μm).

effect, in conjunction with the common occurrence of metal in most meteorite classes, and the presence of meteorites with similar metal-silicate assemblages collectively suggest that red-sloped asteroid spectra that exhibit mafic-silicate absorption bands are indicative of mafic silicate plus metal assemblages. It should be noted, however, that the spectra of iron meteorites exhibit a range of slopes and spectral curvatures, from strongly reddened to weakly reddened and from nearly linear to sharply curved (*Gaffey,* 1976; *Britt and Pieters,* 1988). Until the nature of these spectral variations are better understood, one should be wary of asserting that NiFe metal on asteroid surfaces should introduce a linear reddening component or that failure to exhibit a linear reddened spectrum is evidence against a NiFe metal component on asteroid surfaces.

As noted above, intimate mixtures of various meteoritically relevant dark or opaque materials with mafic silicates can alter our ability to successfully derive mafic silicate abundances and compositions. Studies of the effects of opaque phases include meteoritic metal, magnetite, amorphous C (lampblack), graphite, coal tar extract, bitumen, silicon carbide, cementite, and wustite (*Cloutis et al.,* 1990b,c). In all cases, the presence of red-sloped accessory phases causes the wavelength position of the reflectance minimum of the mafic silicate absorption band in the 1-μm region to shift to shorter wavelengths, with the magnitude of the shift increasing with increasing content of the red-sloped phase; shifts of up to 0.080 μm have been produced. However, when a straight-line continuum (tangent to the reflectance spectrum on either side of this absorption band) is divided out of the spectrum, the wavelength position (center) of the absorption band is restored to its original wavelength position to within ±0.005 μm or less. This allows the composition of the mafic silicates to be retrieved even in the presence of abundant (many tens of percent) red-sloped phases such as meteoritic Fe. Spectrally flat opaque phases generally have less of an effect on band positions. Band areas and depths, on the other hand, are more strongly affected by the presence of nonmafic components, either red sloped or spectrally flat (e.g., *Moroz and Arnold,* 1999).

In some cases, the presence of a particular mineral is determined by a process of elimination. Most E-class asteroids are characterized by high reflectance (>40%) and relatively featureless spectra (*Zellner,* 1975; *Gaffey et al.,* 1992). These characteristics severely limit the range of potential surface mineralogies, since there are few geologically plausible meteoritic or asteroidal materials with high reflectance and featureless reflectance spectra in the 0.3–2.5-μm region (e.g., *Kelley and Gaffey,* 2002). When combined with the presence of meteorites with similar spectral properties (aubrites) and other factors, this strongly suggests the surfaces of these asteroids are dominated (both spectrally and compositionally) by an Fe-free or Fe-poor enstatite.

3.4. "Space Weathering" and Mineralogical Interpretations of Asteroid Spectra

One of the complicating factors in the interpretation of asteroid spectra has been the issue of space weathering and its potential to modify the spectrum (e.g., *Clark et al.,* 2002). "Space weathering" is the catchall term for the process or processes that modify the optical properties of surfaces of atmosphereless bodies exposed to the space environment. The importance of space weathering on the Moon was well documented by the examination of the first lunar samples returned by the Apollo missions (e.g., *Adams and McCord,* 1971). The spectra of lunar soils exhibited systematically lower albedos, weaker mineral absorption features, and redder spectral slopes than the bedrock lithologies from which they were derived (e.g., *Pieters et al.,* 1993). (In the jargon of lunar and asteroidal spectrophotometry, "red," "reddish," and "redder" all refer to spectra whose reflectance increases with increasing wavelength across the visible and/or NIR interval. Such samples are seldom — if ever — visually red as perceived by the human eye.)

Based on the detailed study of lunar soil samples, a physical model for space weathering has been outlined in a series of recent papers (*Pieters et al.,* 2000; *Noble et al.,* 2001; *Taylor et al.,* 2001). The mechanism involves the presence of tiny (4–30 nm) metallic-Fe grains (nanophase metallic Fe, or $npFe^0$) in thin layers or patinas of glass preferentially

coating the surfaces of the finest size fraction of the lunar soil. These grain coats are produced either by condensation of soil minerals vaporized by micrometeorite impacts into the soil and/or by deposition of atoms sputtered off of soil grains by solar-wind particles (e.g., *Hapke,* 2000). Those investigators make a cogent and persuasive case for the proposed mechanism as the process that alters the optical and spectral properties of the lunar soil. However, it was also concluded that this mechanism was important on asteroid surfaces and that it potentially allowed large numbers of ordinary chondrite parent bodies to be present in the asteroid belt (*Pieters et al.,* 2000; *Hapke,* 2000).

The issue of space weathering has been an area of considerable contention among asteroid scientists (e.g., *Gaffey et al.,* 1993a; *Chapman,* 1996; *Clark et al.,* 2002, and references therein). The issue arises from an apparent paradox. Although ordinary chondrites account for the major fraction (~75%) of meteorites falling to Earth, it was recognized very early that few — if any — main-belt asteroids spectrally resembled ordinary chondrites. To explain this discrepancy, space weathering was invoked to optically alter the surface of what were expected to be common ordinary chondrite-type asteroids so as to produce the spectral mismatch. Thus asteroidal space weathering was invoked to reconcile an expectation (that ordinary chondrites were from a common type of asteroid) with an observation (that few — if any — asteroids actually exhibited ordinary chondritelike spectra).

There is clear evidence from telescopic observations for optical alteration of asteroidal surfaces (e.g., *Gaffey et al.,* 1993c). The *Galileo* flyby of 243 Ida and the *NEAR Shoemaker* rendezvous with 433 Eros have reinforced that conclusion, but have also complicated the situation, since the alteration differs between the two asteroids and both differ from the Moon. In the case of the Moon, increased weathering produces weakened absorption features, lowered albedos, and significant color changes. For Ida, there are significant color variations but virtually no albedo variations. Eros exhibits the opposite pattern, with virtually no color variations and large albedo variations. The "space weathering" process(es) occurring on asteroid surfaces are not simply a weakened form of lunar-style space weathering. Moreover, the type of weathering process can clearly vary between otherwise grossly similar bodies (i.e., Eros and Ida are both S-type asteroids).

The real issue is the degree to which "space weathering" affects the interpretation of asteroidal spectra. In spectral-matching methodology, such spectral modification is potentially devastating since it makes the spectral properties of the surficial layer of an asteroid different from that of the substrate and can therefore produce a spurious result if such effects are not considered. The use of spectral parameters (e.g., band centers, BARs) as outlined in previous sections of this chapter appears to mitigate space-weathering effects (e.g., *Gaffey,* 2001; *Hapke,* 2001). Based on preliminary analysis of lunar samples, *Gaffey* (2001) notes that the diagnostic parameters are essentially unchanged until a high degree of weathering is reached, a level generally beyond that proposed or observed on asteroid surfaces. So while "space weathering" can alter asteroid surfaces, making the spectra redder and weakening the absorption features, it does not appear to significantly impact the mineralogical interpretations of those spectra. This is consistent with the generally similar results of the analysis of the NIR spectra (affected by space weathering) and the X-ray/γ-ray spectra (unaffected by space weathering) from the *NEAR Shoemaker* observations of Eros (*McCoy et al.,* 2001).

3.5. Importance of Laboratory Spectral Studies

While the field of asteroid research has made many important advances in determining mineralogies for a number of asteroids, particularly from analysis of reflectance spectra (e.g., *McCord et al.,* 1970; *Gaffey et al.,* 1993a; *Gaffey and Gilbert,* 1998; etc.), the fact remains that for a distressingly large number of asteroids, surface mineralogies are poorly constrained, and even when mineralogies can be approximated, widely different interpretations of parent-body history and evolution can often be accommodated by available data. Some mafic-silicate-dominated assemblages, such as 433 Eros (*Veverka et al.,* 2000) are consistent with either partially differentiated (i.e., primitive achondrites analogous to lodranites, winonaites, and acapulcoites) or undifferentiated assemblages (i.e., ordinary chondrites). Even when high-quality spectral data are available and supplemented by elemental-abundance information, as is the case for Eros, this uncertainty may still not be resolvable (*Trombka et al.,* 2000; *Veverka et al.,* 2000; *McCoy et al.,* 2001). However, interpretation of the observational spectral data in light of relevant laboratory spectral data and/or rotationally resolved spectral observations can be used to resolve the differentiated nature of an S-class asteroid (*Gaffey,* 1984).

To a significant extent the paucity of detailed mineralogic interpretations and the ambiguity associated with many interpretations arises from the limitations in or the lack of appropriate interpretive calibrations. Such calibrations are largely derived from laboratory spectral studies of meteorites and mineral mixtures intended to simulate asteroid lithologies. For example, the need for a systematic spectral study of olivine, low-Ca pyroxenes, and high-Ca pyroxenes was noted above. Similarly, the spectral behavior of NiFe metal needs to be better understood. The behavior of NiFe metal in assemblages depends on the petrologic associations. For example, the metal in undifferentiated (i.e., ordinary chondrite) meteorites is spectrally neutral (*Gaffey,* 1986), while Fe from differentiated meteorites is invariably red-sloped when measured (*Gaffey,* 1976; *Britt and Pieters,* 1988; *Cloutis et al.,* 1990a, and references therein). It has been speculated that the metal grains in chondrites are coated with an optically thick alteration layer that suppresses the spectral signature of the metal (e.g., *Gaffey,* 1986), but

an actual spectroscopic/petrologic study is needed to understand this effect.

In addition, gas-rich and shock-blackened meteorites, inferred to have been exposed at the surface of their parent bodies at some point in their histories, do not show evidence for spectral reddening, as would be expected for many of the space-weathering mechanisms that have been proposed (*Britt and Pieters,* 1991a,b; *Keil et al.,* 1992). Instead, these "space-weathering" effects generally result in reductions in overall reflectance and mafic-silicate absorption-band depths. One important result to note is that the reflectance spectra of many S-class asteroids have been successfully reproduced by numerical mixing models using various combinations of meteoritic metal plus mafic silicates (e.g., *Hiroi et al.,* 1993). It would be very valuable to confirm the validity of such mixing models with spectral measurements of corresponding physical mixtures.

3.6. Nature of the 3-μm Absorption Feature

The reported presence of an absorption feature in the 3-μm region of many asteroid spectra (e.g., *Rivkin et al.,* 2000, and references therein) has received much attention recently because of its potential importance as an indicator of "hydration." This wavelength interval is of importance for asteroid research because the fundamental O-H stretching bands of H_2O/OH occur in this region. Characteristics of absorption features in this region, such as wavelength position, the number and shapes of the absorption bands, and their relative intensities, can be used to distinguish a range of geological materials as well as provide information on the speciation of H_2O/OH (*McMillan and Remmele,* 1986; *Clark et al.,* 1990; *S. J. Gaffey et al.,* 1993).

For some asteroid types, a 3-μm "water" feature is expected based on the presence of hydrated mineral species in their best meteorite analogs. The presence of such a feature in many low-albedo asteroid types (e.g., C-, B-, and G-types) is important supporting evidence for the validity of metamorphic types 1 and 2 carbonaceous chondrites as analogs to the surface material of these asteroids. Asteroids 1 Ceres and 2 Pallas are examples of objects with strong 3-μm features in their spectra (e.g., *Jones et al.,* 1990; *Rivkin et al.,* 2002). Thus this is an important wavelength region for providing critical insights into asteroid surface compositions. However, 3-μm features have also been reported in asteroids whose most plausible meteoritic analogs are anhydrous assemblages (e.g., *Rivkin et al.,* 1995, 2000, 2002). This has led to a reevaluation of the significance of the 3-μm feature in asteroid spectra.

There are observational difficulties (e.g., telluric water vapor absorptions, low reflectance) associated with obtaining reliable spectra in this wavelength region. The simple presence of a 3-μm absorption band has often been interpreted as indicative of "hydration" or widespread aqueous alteration (e.g., *Merényi et al.,* 1997; *Rivkin et al.,* 1995, 2000, 2001; *Howell et al.,* 2001). However, a number of plausible alternative explanations are also possible. These include materials normally considered to be anhydrous (such as mafic silicates) containing structural OH (*Miller et al.,* 1987; *Ingrin et al.,* 1989; *Skogby and Rossman,* 1989; *Skogby et al.,* 1990), the presence of fluid inclusions (*Roedder,* 1984; *Zolensky et al.,* 1999a,b), the presence of xenolithic hydrous meteorite components on asteroid surfaces from impacts (e.g., *Lovering,* 1962; *Binns,* 1969; *Wilkening,*1977; *Neal and Lipschutz,* 1981; *Keil,* 1982; *Nozette and Wilkening,* 1982; *Rubin and Keil,* 1983; *Sears et al.,* 1983; *Verkouteren and Lipschutz,* 1983; *Yanai et al.,* 1983; *Bunch and Rajan,* 1988; *Lipschutz et al.,* 1988; *Scott et al.,* 1989; *Pellas,* 1991; *Zolensky et al.,* 1991, 1993; *Buchanan et al.,* 1993a,b), and solar-wind-implanted H (*Starukhina,* 2001), or the presence of troilite, which also exhibits an absorption feature in the 3-μm region (*Vaughan and Craig,* 1978). All these processes can give rise to absorption features in the 3-μm region in otherwise "anhydrous" lithologies. Band depths in the 3-μm region of asteroid spectra, which range up to 50% (and up to 88% in one case) (*Larson et al.,* 1983; *Merényi et al.,* 1997; *Rivkin et al.,* 2000, 2002) are consistent with all of these alternative mechanisms.

Available meteorite reflectance spectra, including a variety of falls and finds (*Miyamoto et al.,* 1989; *Miyamoto,* 1991; *Salisbury et al.,* 1991; *Miyamoto and Zolensky,* 1994), indicate that band depth in the 3 μm region in meteorite spectra, including recent falls, can range up to 30% for H_2O/OH contents as low as 0.1 wt%. Reflectance and transmittance spectra of "anhydrous" meteorites such as achondrites, E- chondrites, and ordinary chondrites (including finds and recent falls) normally exhibit absorption bands in the 3-μm region attributable to O-H stretching vibrations (*Sandford,* 1984; *Miyamoto,* 1987, 1990, 1991; *Wagner et al.,* 1988; *Miyamoto et al.,* 1989; *Salisbury et al.,* 1991; *Miyamoto and Zolensky,* 1994; *Bishop et al.,* 1998a,b). The presence of 3-μm absorption features due to adsorbed atmospheric water in the spectra of otherwise anhydrous samples simply emphasizes the minute quantity of water required to produce a 3-μm absorption feature in a spectrum.

Numerous meteorite regolith breccias are mixtures of anhydrous (achondritic) and hydrous (e.g., carbonaceous chondrite) clasts (e.g., *Lovering,* 1962; *Binns,* 1969; *Wilkening,* 1977; *Neal and Lipschutz,* 1981; *Keil,* 1982; *Nozette and Wilkening,* 1982; *Rubin and Keil,* 1983; *Sears et al.,* 1983; *Verkouteren and Lipschutz,* 1983; *Yanai et al.,* 1983; *Bunch and Rajan,* 1988; *Lipschutz et al.,* 1988; *Scott et al.,* 1989; *Pellas,* 1991; *Zolensky et al.,* 1991, 1993; *Buchanan et al.,* 1993a,b). The asteroid belt is a dynamic environment and a perception of asteroid surfaces as being simple, pristine assemblages is oversimplified. Mixing of different materials and incorporation of widely different assemblages into asteroid regoliths is probably the norm rather than the exception. Thus we should expect some anhydrous (differentiated) asteroids to show evidence for a 3-μm "water" absorption band due to this dynamical mixing. *Starukhina* (2001) has discussed the formation of hydroxyl groups by interaction of

solar-wind protons with O atoms in regolith particles. Those calculations indicate that reasonable concentrations of solar-wind H-produced hydroxyl groups in a regolith could produce the 3-μm band depths seen in many asteroids.

This discussion emphasizes the difficulties that can arise in the interpretation of a 3-μm spectral feature and the importance of carrying out such interpretations in a solid geologic and meteoritic context. As observational data for the 3-μm region improve (e.g., *Rivkin et al.,* 2001) the fine structure in this wavelength region can be used to distinguish between the various interpretations listed above and identify the specific "water-bearing" species (e.g., *Bishop et al.,* 1994).

3.7. Identification of Minerals on the Basis of Multiple Spectral Features

Identifying specific minerals on asteroid surfaces from reflectance spectra must be approached cautiously. Our confidence in mineralogical interpretations increases as the number of unique or diagnostic absorption features (not necessarily the number of absorption bands) increases.

As an example, the surface mineralogies of the A-class asteroids are generally interpreted as indicating olivine-rich assemblages (*Cruikshank and Hartmann,* 1984). This is based on the presence of a single absorption feature near 1.05 μm. A number of other minerals also exhibit an absorption band in this region, notably pyroxene (*Cloutis and Gaffey,* 1991a). However, the "shape" of this feature (i.e., evidence for side lobes near 0.85 and 1.2 μm), the lack of associated absorption features in the 2-μm region, the widespread presence of olivine in the inner solar system, and a number of olivine-rich meteorites in our collections, present strong collective evidence for the correctness of this interpretation. The complete surface mineralogies of these asteroids are still uncertain, however. The asteroid spectra do not match the reflectance spectra of pure olivine in all details, particularly in terms of overall slope. A number of possible factors may account for this spectral mismatch, including the presence of metal, chromite, temperature differences between laboratory and asteroid spectra (*Lucey et al.,* 1998; *Moroz et al.,* 2000), or "space weathering."

Interpretations of asteroid reflectance spectra must also be internally consistent. As an example, assigning a 3-μm absorption feature to a specific hydrated phase has certain implications. These include the expected presence of accompanying H_2O/OH overtone and combination bands in the 1.4- and/or 1.9-μm regions, which should persist even when hydrated minerals are exposed to the space environment (*Bishop and Pieters,* 1995). These overtone bands are generally an order of magnitude less intense than the 3-μm O-H stretching fundamental band and the depth of these overtone/combination bands can be further reduced by the presence of opaque minerals, or if they lie in a region of low overall reflectance; thus they may not always be detectable. However, if the asteroid albedo is moderate or high (e.g., >15%), a hydrated assemblage should exhibit detectable 1.4- and 1.9-μm features. If these hydrated minerals are also Fe-bearing, we would also expect additional absorption bands in the 0.4–0.9-μm region to be present (e.g., *Vilas et al.,* 1994).

4. MINERALOGICAL CHARACTERIZATIONS OF ASTEROIDS

Over the past two decades there has been a slow but steady improvement in both the quality of asteroid spectral data and in the interpretive methodologies and calibrations used to analyze that data. It is useful to summarize the present status of detailed mineralogical interpretations of asteroids as well as the advances that have been made in such interpretations in the 13 years since the *Asteroids II* volume was published. The mineralogical characterizations of specific asteroids are listed in Table 3.

4.1. S-type Asteroids

The analysis of S-asteroid survey spectra by *Gaffey et al.* (1993a) made the first detailed application of the phase-abundance calibration of *Cloutis et al.* (1986). The results showed the diversity of lithologies present within this single taxonomic type. *Gaffey et al.* (1993a) identified seven mineralogical subtypes of the S-taxon, where the silicate assemblages ranged from nearly monomineralic olivine [subtype S(I)] through basaltic silicates [subtype S(VII)]. Of the seven subtypes, only one [subtype S(IV)] did not require igneous processing to produce the observed assemblage. *Gaffey et al.* (1993a) concluded that at least 75% — and probably >90% — of the S-type asteroids had experienced at least partial melting within their parent bodies. This result strongly contradicted the commonly held notion (e.g., *Anders,* 1978; *Wetherill and Chapman,* 1988) that most S-asteroids must be undifferentiated ordinary chondrites (modified by space weathering) in order to account for the preponderance of ordinary chondrites among meteorite falls. However, this result was consistent with the evidence that a large majority of the meteorite parent bodies experienced high temperatures and underwent at least partial differentiation (e.g., *Keil,* 2000).

4.2. 6 Hebe

Of particular interest was subtype S(IV), which could (but was not required to) include undifferentiated assemblages such as ordinary chondrites. This significantly narrowed the field of candidates as potential ordinary chondrite parent bodies. Combined with improved understanding of meteorite delivery mechanisms (e.g., *Farinella et al.,* 1993a,b; *Morbidelli et al.,* 1994; *Migliorini et al.,* 1997), these results allowed *Gaffey and Gilbert* (1998) to identify asteroid 6 Hebe as the probable parent body of both the H chondrites and the IIE iron meteorites. There was also significant skepticism concerning the "H-chondrite + metal" assemblage invoked in the paper (e.g., *Keil,* 2000). Therefore, the fall of the Portales Valley meteorite was particularly timely. Portales Valley consists of masses of H6 chondrite either

TABLE 3. Mineralogically characterized asteroids.

Asteroid	Class	Diameter	a (AU)	Family	Predicted Mineralogy (Meteorite Affinity)*	Reference
3 Juno	S(IV)	244	2.670	N	Px/(Ol + Px) ~ 0.30 (possible L chondrite)	1†
4 Vesta	V	~570 × 460	2.362	Y	Pyroxene-plagioclase basalt (HED meteorites)	2
Vesta Family	V/J	—	—	Y	Range of HED lithologies	3,19,20
6 Hebe	S(IV)	185	2.426	N	Px/(Ol + Px) ~ 0.4 and NiFe metal (H chon, IIE irons)	4
7 Iris	S(IV)	203	2.386	N	Px/(Ol + Px) ~ 0.30, Px ~ $Fs_{42}Wo_7$ or Cpx-bearing (possible L chondrite)	1†
8 Flora	S(III)	141	2.201	Y	Px/(Ol + Px) ~ 0.25, NiFe metal, Fe-rich Px and/or Ca-rich Px	5
9 Metis	S(I)	168–210	2.386	Y	Px/(Ol + Px) ~ 0.12 and NiFe metal	6
11 Parthenope	S(IV)	162	2.452	N	Px/(Ol + Px) ~ 0.34	1†
12 Victoria	S(II)?	117	2.334	Y	Px/(Ol + Px) ≤ 0.14 and NiFe metal	1†
15 Eunomia	S(III)	272	2.644	Y	Ol + NiFe + (low-Ca Px) to high-Fe and Ca Px basalt	7
16 Psyche	M	264	2.922	N	NiFe metal	8
17 Thetis	S	93	2.469	N	Px/(Ol + Px) ~ 0.54 or low-Ca Px: Calcic Px ~ 60:40 and Ol <15%	22†
18 Melpomene	S(V)	148	2.296	N	Px/(Ol + Px) ~ 0.47	1†
20 Massalia	S(VI)	151	2.408	Y	Px/(Ol + Px) ~ 0.66, Px ~ $Fs_{26}Wo_4$	1†
25 Phocaea	S(IV)	78	2.400	N	Px/(Ol + Px) ~ 0.30	1†
26 Proserpina	S(II)	99	2.656	N	Px/(Ol + Px) ~ 0.30	1†
27 Euterpe	S(IV)		2.347	N	Px/(Ol + Px) ~ 0.25	1†
37 Fides	S(V)	112	2.642	Y	Px/(Ol + Px) ~ 0.72 ± 0.17	1†
39 Laetitia	S(II)	159	2.769	Y	Px/(Ol + Px) ~ 0.26	1†
40 Harmonia	S(VII)	111	2.267	N	Px/(Ol + Px) ~ 0.89 (0.68–1.0), Px ~ $Fs_{27}Wo_9$	1†
42 Isis	S(I)	107	2.441	Y	Px/(Ol + Px) ~ 0.0 and NiFe metal(?)	1†
43 Ariadne	S(III)	65	2.203	Y	Px/(Ol + Px) ~ 0.13–0.20	1†
44 Nysa	E	73	2.422	Y	Nearly Fe-free enstatite (<Fs_1)	9
63 Ausonia	S(II–III)	108	2.395	Y	Px/(Ol + Px) ~ 0.27 and NiFe metal(?)	1†
67 Asia	S(IV)	60	2.421	N	Px/(Ol + Px) ~ 0.46	1†
68 Leto	S(II)	127	2.782	Y	Px/(Ol + Px) ~ 0.18	1†
80 Sappho	S(IV)	82	2.296	N	Px/(Ol + Px) ~ 0.30	1†
82 Alkmene	S(VI)	64	2.765	N	Px/(Ol + Px) ~ 0.61 ± 0.16; Px ~ $Fs_{23}Wo_2$	1†
113 Amalthea	S(I–II)	48	2.376	Y	Px/(Ol + Px) ~ 0.13, Px ~ $Fs_{34}Wo_{14}$ and NiFe metal (?)	6,10
115 Thyra	S(III–IV)	84	2.380	Y	Opx + Ca Px assemblage indicated	1‡
215 Kleopatra	M	217 × 94 × 81	2.767	N	NiFe metal	11
246 Asporina	A	64	2.695	N	Olivine + NiFe metal(?) (possible pallasite)	12,13
289 Nenetta	A	42	2.874	N	Olivine + NiFe metal(?); Px/(Ol + Px) < 0.05 (possible pallasite)	1†,13
349 Dembowska	R	140	2.925	Y	Px/(Ol + Px) ~ 0.45; Px ~ $Fs_{25}Wo_{10}$	14
354 Eleonora	S(I)	162	2.796	N	Px/(Ol + Px) ~ 0.05	1†
387 Aquitania	S	106	2.742	Proposed	Spinel (in abundant CAIs?) (CV or CO chondrite)	15
433 Eros	S(IV)	39 × 13 × 13	1.458	N	Px/(Ol + Px) ~ 0.36; Px ~ $Fs_{42}Wo_{18}$ or Cpx-bearing (possible LL chondrite)	16,21
446 Aeternitas	A	43	2.788	Y	Olivine + NiFe metal (?); Px/(Ol + Px) < 0.05 (possible pallasite)	1†,12,13
532 Herculina	S(III)	231	2.772	N	Opx + Ca Px assemblage indicated	1‡
584 Semiramis	S(IV)	56	2.374	Y	Px/(Ol + Px) ~ 0.26 + NiFe metal(?); Px ~ $Fs_{42}Wo_{16}$	1†
674 Rachele	S(VII)	101	2.924	N	Px/(Ol + Px) ~ 0.68–1.0	1†
847 Agnia	S	32	2.783	Y	Low-Ca Px: Calcic Px ~ 60:40; Ol < 15%	22
863 Benkoela	A	32	3.200	N	Olivine + NiFe metal (?) (possible pallasite)	13
980 Anacostia	S	89	2.741	Proposed	Spinel (in abundant CAIs?) (CV or CO chondrites)	15
1036 Ganymed	S(VI–VII)	41	2.662	N	Px/(Ol + Px) ~ 0.64–0.82; Px ~ $Fs_{34}Wo_4$	1†
3103 Eger	E	1.5	1.406	N	Iron-free enstatite	17
1986 DA	M	2.3	2.811	N	NiFe metal	18

*Except where otherwise noted, "Px" indicates a low-Ca orthopyroxene.
†Mineral abundances and compositions using spectral parameters from *Gaffey et al.* (1993a) and equations (2)–(4) and Fig. 4 from the present paper.
‡Olivine-poor or olivine-free two-pyroxene assemblage indicated by test described in text.

References: (1) *Gaffey et al.* (1993a); (2) *Gaffey* (1997); (3) *Binzel and Xu* (1993); (4) *Gaffey and Gilbert* (1998); (5) *Gaffey* (1984); (6) *Kelley and Gaffey* (2000); (7) *Reed et al.* (1997); (8) *Ostro et al.* (1985); (9) *Gaffey et al.* (1993b); (10) *Gaffey* (2002); (11) *Ostro et al.* (2000); (12) *Hiroi et al.* (1993); (13) *Lucey et al.* (1998); (14) *Abell and Gaffey* (2000); (15) *Burbine et al.* (1992); (16) *McFadden et al.* (2001); (17) *Gaffey et al.* (1992); (18) *Ostro et al.* (1991); (19) *Hiroi et al.* (1995); (20) *Vilas et al.* (2000); (21) *McCoy et al.* (2001); (22) *Sunshine et al.* (2002).

embedded in a NiFe metal matrix or crosscut by large (centimeter-scale) metal veins (e.g., *Kring et al.,* 1999; *Pinault et al.,* 1999; *Rubin and Ulff-Møller,* 1999; *Ruzika et al.,* 1999). Although there are still questions concerning the exact mechanism(s) that melted the metal and mixed the H-chondrite masses and the molten metal, there can no longer be any doubt that assemblages actually exist like that invoked for the Hebe surface by *Gaffey and Gilbert* (1998).

It was of course fortuitous that the identification of Hebe as the probable parent body of the H chondrites and the

IIE iron meteorites was followed so closely by the fall of the Portales Valley meteorite. In the search for meteorite parent bodies, one seldom has such a strong piece of supporting evidence provided in such a timely manner. The linkage of a major meteorite group (~32% of meteorite falls) to specific location in the asteroid belt now allows us to place these meteorites — and the detailed chemical and chronological information that they provide — into a spatial context in the early solar system, and in turn, to place temporal and chemical constraints on that specific location in the asteroid belt.

4.3. Spinel-bearing S-type Asteroids

Two spectrally anomalous bodies (387 Aquitania and 980 Anacostia) were identified during the analysis of S-asteroid survey data. Analysis of these two spectra (*Burbine et al.,* 1992) indicated a spectrally significant spinel component, and it was proposed that the spinel was associated with a high abundance of Allende-type white inclusions, indicating accretion at an early stage of nebular cooling. Because of similarities in orbital elements, it was further suggested that these two mineralogically distinctive bodies were fragments of a single parent body, i.e., a "compositionally detected" family. Such a genetic family would be far below the detection limit of any dynamical family identification system yet presented.

4.4. 4 Vesta

Gaffey (1997) used rotational spectral variations to map the large-scale lithologic variations across the surface of Vesta. The lithologies range from diogenite to eucrite, suggesting a largely intact crust (eucrites) with lower crustal units (diogenites) exposed — presumably by impact structures — in several regions. Hubble Space Telescope multicolor imagery (*Binzel et al.,* 1997) shows appropriate color variations across the surface corresponding to the spectrally derived lithologic map.

4.5. Vesta Family Objects

An extensive investigation of small objects in the Vesta family (*Binzel and Xu,* 1993) shows spectra very similar to that of Vesta itself. (Some of these bodies are not members of the dynamical Vesta family, but their distinctive spectra strongly indicate they are members of the "true" or genetic Vesta family.) Although the CCD spectral coverage was inadequate to obtain actual mineralogical characterizations, the close similarity to the very distinctive Vesta spectrum leads to a robust conclusion that the family members are HED assemblages. Apparent differences in the portion of the 1-μm feature available in the CCD spectral interval were noted and attributed to different HED lithologies.

Hiroi et al. (1995) use a curve-fitting routine to define several parameters [band center (actually band minimum), band depth, and band width] of the partially sampled 1-μm band in the CCD spectra of a number of Vesta family objects. They show a range in band positions twice the range of band position they measured in a set of HED meteorites [but very comparable to the range of band positions for HEDs shown by *Gaffey* (1997)], consistent with these bodies sampling a range of HED lithologies. However, the incomplete and variable coverage of the 1-μm band and the use of band minimum instead of band center make a more detailed comparison between individual family members difficult.

Vilas et al. (2000) identify a narrow feature centered at 0.5065 μm suggestive of a high-Ca pyroxene component (augite) that varied between different Vesta family members. This is consistent with different HED lithologies, since eucrites have more Ca-rich pyroxenes than diogenites.

Burbine et al. (2000) interpret ~0.44 to ~1.65 μm spectra of vestoids, both within and outside the dynamically defined Vesta family. Based primarily on the wavelength position of the reflectance maximum near 1.4 μm, they conclude that all of these spectra were consistent with surface compositions similar to eucrites and howardites, and none of them were similar to diogenites. Extension of vestoid spectral observations to 2.5 μm should allow testing of the presence or absence of diogenite-type assemblages and would provide robust constraints on excavation depth within the crust of the parent body, Vesta.

Kelley et al. (2001b, 2002) present the first detailed mineralogical analysis of a vestoid (1929 Kollaa) with spectral coverage extended to 2.5 μm. They conclude that the mineralogy of Kollaa is consistent with an HED-type assemblage as expected, and more specifically that it indicates a cumulate eucrite-type assemblage. Such an assemblage would form deep in the eucritic upper layer of the Vesta crust.

The Vesta family emphasizes the need to specify the type of "family" being discussed. *Farinella et al.* (1992) drew attention to the inherent ambiguities in the use of the term "family" when referring to asteroid groupings derived from different criteria. They suggest that the term "family" should be reserved for groupings passing both statistical and taxonomic/spectroscopic tests that should be genetic associations. These can be presumed to have a common origin in a single parent body. Based on spectral criterion, we would argue that all of the vestoids (identified by their characteristic spectra) in the Vesta region should be considered members of the Vesta family. The distinction between vestoids within and outside the dynamically defined Vesta family is relevant only so far as it provides a potentially powerful dataset to refine our understanding of the initial distribution and/or the dynamical evolution of bodies within a genetic family.

4.6. 9 Metis

Kelley and Gaffey (2000) show that the surface assemblage of Metis was dominantly olivine-rich mafic silicates [ol/(ol + px) ~ 0.88] and NiFe metal. Based on the similarity of orbital elements and sharing an uncommon S-asteroid mineral assemblage, they conclude that Metis and 113 Amalthea were genetically related and were the largest surviving fragments of a disrupted parent body (asteroid family).

4.7. 15 Eunomia

Reed et al. (1997) use simultaneous visible and thermal IR lightcurve observations of Eunomia to derive the body shape and albedo variability of this asteroid. They show that the NIR spectrum of Eunomia varies substantially on opposite ends of this "almond-shaped" body. The spectrum of the "pointy" end indicates abundant olivine and metal with lesser pyroxene, predominately low-Ca. The "rounded" end is more basaltic and contains abundant high-Fe and high-Ca pyroxene. Eunomia appears to expose a crust-to-core cross-section of its parent body.

4.8. 3103 Eger (1982 BB)

Based on a high albedo and a relatively featureless spectrum, near-Earth asteroid (NEA) 3103 Eger was identified as Fe-free enstatite (*Gaffey et al.,* 1992). Based upon the uniqueness of this assemblage in the NEA population and meteorite fall patterns, it was concluded that Eger is the probable parent body of the enstatite achondrite meteorites (aubrites) and is itself derived from the Hungaria region of the innermost asteroid belt.

4.9. Iron Alteration Minerals and Phyllosilicates in Dark Asteroids

Weak visible region features in CCD spectra of low albedo asteroids have been detected and confirmed by Vilas and coworkers (*Vilas and Gaffey,* 1989; *Vilas et al.,* 1993; *Vilas et al.,* 1994). These features are indicative of a number of minerals (e.g., the clay mineral, antigorite) and Fe-alteration products consistent with the mineralogy present in various CI1 and CM2 carbonaceous chondrites. Although considerable work remains, especially in the spectral study of the carbonaceous chondrite mineral phases, it is evident that this type of investigation is the key to unraveling the undoubtedly complex mineralogy of the dark asteroids.

5. IMPLICATIONS FOR ASTEROID FAMILY STUDIES

5.1. Types of Asteroid Families

One area of asteroid research in which detailed mineralogical characterizations are at the forefront is the study of asteroid families. Clusters of asteroids in similar orbits, or "families," were first recognized nearly a century ago (*Hirayama,* 1918). Depending on the dynamical and statistical or subjective criteria used, the number of proposed families ranges from about 6 to more than 100 (e.g., *Hirayama,* 1933; *Brouwer,* 1951; *Arnold,* 1969; *Kozai,* 1979; *Williams,* 1989, 1992; *Zappalà et al.,* 1990, 1994, 1995). From the outset, it was suggested that most asteroid families resulted from cataclysmic collisions between asteroids resulting in the breakup of individual parent bodies.

In the present paper, we explicitly define an "asteroid family" (aka "genetic family") as the fragments of a partially or completely disrupted parent body. This is an idealized definition that may not be testable in many situations. Thus, families can include a large number of fragments of their parent body, or families may be depleted to the point where only a few fragments remain. Accordingly, there are different types of asteroid families based on the criteria used to establish or study the family (e.g., dynamical families, taxonomic families, mineralogical families, etc.).

Dynamical families are clusters of asteroids identified in proper orbital-element space (e.g., *Zappalà et al.,* 1990, 1994, 1995; *Williams,* 1992). There are significant disagreements on the total number of such families, their memberships, and the criteria and techniques used to identify them. However, it is also highly probable that statistically well-defined dynamical families are true genetic families.

Physical studies of families to test whether their members are "truly" related began with studies of their broadband colors (*Gradie and Zellner,* 1977). Investigations based on visible wavelength spectral properties and taxonomy use dynamical families as a starting point for making assessments of the "reality" of families (e.g., *Chapman,* 1987; *Bell,* 1989; *Chapman et al.,* 1989; *Granahan,* 1993; *Bus,* 1999). The tacit assumption is that a family generated by collisional breakup of a parent body will be composed of fragments of one taxonomic type or of compatible taxonomic types. These studies have been used to identify probable interlopers in families.

In addition, the goal of detailed mineralogic studies is to recognize genetic ("true" or "real") families, and such studies similarly use dynamical families as a starting point. This approach makes assessments of family membership based on the presence of mineralogical assemblages consistent with derivation from a single parent body. A goal of such studies of genetic asteroid families is to reveal uniquely preserved information that may help to unlock the secrets of the timing of particular events in the early solar system and its subsequent history. The presence and nature of collisionally produced genetic asteroid families can provide important constraints on the processes involved in the disruptions of large (~100–1000 km) bodies, the collisional lifetime of asteroids as a function of size and composition, the thermal history and internal compositional structure of their parent bodies, and the rate of orbital diffusion of families.

Historically, most tests of asteroid family membership have relied on taxonomy over visible wavelengths (e.g., *Chapman,* 1987; *Bell,* 1989; *Chapman et al.,* 1989; *Granahan,* 1993). The work of *Bus* (1999) and *Bus et al.* (1996) combine both visible wavelength spectra and spatial location (within each grouping) to examine the likely membership and extent of a number of small families, where good consistency between spectral characteristics and location is found in each case. Further studies are now extending family member spectral measurements into the NIR out to ~1.6 μm (e.g., *Carvano et al.,* 2001; *Burbine et al.,* 2000), where the consistency of spectral characteristics remains strong. It is important to emphasize that the similarity of observational characteristics does not "prove" a family relationship, nor does taxonomic dissimilarity "disprove" a

family relationship. The next progressive step for investigating the "reality" of dynamical or suggested families is the study of their detailed mineralogical and compositional properties. Such studies can more rigorously test whether a potential family is compatible with derivation from a common parent body and can establish whether it is a probable genetic family.

It is important to realize the implications of the large number of magmatic iron meteorite types (e.g., *Keil,* 2000) for asteroid family studies. The large number of iron meteorite parent bodies constrains the minimum number of parent-body disruption events (family-forming events) that have occurred during solar-system history. Currently there are ~25 recognized dynamical families that appear to have been produced by collision disruption and partial-to-complete dispersal of their parent bodies (e.g., *Marzari et al.,* 1999). Most of the potential dynamical families surveyed by *Bus* (1999) were considered valid because they were spectrally similar and spectrally distinct from the background objects. Spectrally homogeneous families such as these are very improbable sources of iron meteorites. Instead, magmatic iron meteorites must represent excavated core material from fully (or extensively) differentiated bodies. The families produced by the disruption of such differentiated bodies should consist of a variety of lithologies (basalts and HED type assemblages, dunites, pallasite-type assemblages, and Fe) and spectral types (V, A, S, M). Such families appear absent among the recognized dynamical families. Thus, most of the >55 families that released the >55 types of magmatic iron meteorites must have been depleted and/or dispersed so that they no longer provide dynamical grouping identifiable by current search techniques. It remains an open question as to whether any of the differentiated material other than the high-strength Fe core samples still exists in a recognizable form in the asteroid belt today. *Burbine et al.* (1996) propose a scenario in which the lower-strength differentiated materials may have been "battered to bits" and entirely or almost entirely removed from the asteroid belt. This model is testable by pushing detailed mineralogical studies to smaller and smaller main-belt asteroids.

If they are detectable at all based on orbital criteria, such depleted and dispersed families could resemble many of the smaller and generally not statistically significant Williams families (*Williams,* 1989, 1992). It has been demonstrated that a detailed compositional study of such small families combining groundbased visible and NIR (~0.4–2.5 μm) spectral data is feasible and can show where probable genetic relationships exist (*Kelley and Gaffey,* 1996, 2000, 2002; *Kelley et al.,* 1994).

Until recently, no dynamical asteroid family had sufficient spectral coverage of its membership to adequately permit compositional testing of its genetic reality. The Family Asteroid Compositional Evaluation Survey (FACES) was created to fill gaps in existing family asteroid spectroscopic databases and to obtain new data on additional family members. To date, the ongoing observational phase of this survey has collected visible and NIR spectroscopic data on more than 150 main-belt asteroids and NEAs. Appropriate data covering the volume or mass majority of several asteroid families have now been assembled.

5.2. Estimating Mass Loss from Asteroid Families and from the Asteroid Belt

When a genetic family originally forms from disruption of its parent body, the mass fractions of different layers (lithologies) within the parent (e.g., NiFe core, olivine mantle, basaltic crust, etc., in a differentiated body) are a function of the chondritic type that made up the raw material of the parent body (e.g., *Gaffey et al.,* 1993a). Since mineralogical investigation of the members of a family can identify the original bulk compositions, the original relative abundance of the different lithologies can be determined. In a highly evolved family, the composition and size of the larger family members can be used to place a lower limit on the parent-body size and hence establish a lower limit on the mass lost from the family (e.g., *Kelley and Gaffey,* 2000). Since even the most evolved families are certainly younger than the solar system, and since the collisional evolution of asteroids is essentially independent of whether or not they are members of families, the mass-depletion factors of the highly evolved families place a lower limit on the mass depletion of the asteroid belt as a whole.

A case in point is the *Williams* (1992; also personal communication, 1992) Metis family. Asteroids 9 Metis and 113 Amalthea represent 98% of the remaining volume of the dynamical Metis family. *Gaffey* (2002) shows that 113 Amalthea is a silicate (olivine + pyroxene) fragment of a parent body that most likely underwent significant differentiation (thermal processing) and represents an uncommon S subtype. *Kelley and Gaffey* (2000) demonstrate that 9 Metis is likely to be the remnant core of its parent body. Metis appears to be metal-rich, but still retains a significant silicate signature matching that of Amalthea. Therefore, this pair of asteroids passes the genetic test: Their silicate assemblages are very similar and quite distinct from most other S asteroids, and they have similar orbital elements. The silicate-mineral abundances (olivine-to-pyroxene ratio) for these asteroids are within the range of abundances that can be derived from igneous processing of CV/CO-, H-, L-, and LL-chondrite meteorite-type parent materials. The ranges of silicate-to-metal ratios of these meteorite groups are well known (e.g., *Brearley and Jones,* 1998). Since Metis appears to preserve the core-mantle boundary, its diameter was used to represent a *minimum* core size (metal fraction) for the parent body. It was then possible to calculate a range of silicate fractions for each of the possible meteorite starting compositions, and hence a range of parent-body diameters for each group. The minimum parent-body diameters ranged from ~330 km to ~490 km across the suite of meteorite analogs. Once the diameter of the parent body was constrained, so is the volume ($v = 4\pi r^3/3$). The volume of material remaining in the family was then calculated using the best diameters available for the individual asteroids. Consequently, a percentage of the remaining volume was determined (total

remaining volume/parent body volume) for each of the possible starting groups. This resulted in a range of remaining volume of only 4–14%. Therefore, it appears that a *minimum* of 86–96% of the original volume of the Metis parent body has been lost over time, or has yet to be identified in the background asteroid population.

Similar exercises are being performed for additional asteroid families in the FACES database. The better the compositional evaluations of individual family members are, the tighter the resulting parent-body constraints will be. Since any genetic family is by definition younger than the asteroid belt, the highest depletion observed among asteroid families sets the lower limit on the overall depletion of the asteroid belt. Current results suggest an initial asteroid belt much more massive than that presently observed, almost certainly >100× as massive and probably >1000× as massive. Additional studies of small (i.e., highly evolved) genetic asteroid families will further constrain this limit.

5.3. Maria Family

Space does not permit a detailed discussion of the mineralogical issues of individual asteroid familes, so the Maria family is used as an example. This family is located adjacent to the 3:1 mean motion resonance with Jupiter and could be an important contributor to the terrestrial-meteorite flux. G. Wetherill (personal communication, 1991) suggests that this family is a good dynamical candidate for an ordinary chondrite source. The survey spectra of several members of this family appear very similar to one another. This would be expected for an undifferentiated, chondritic parent body. Based upon a dynamical investigation, *Zappalà et al.* (1997) identify the Maria family as the most promising potential source of the two largest NEAs, including 433 Eros, which was the target of NASA's *NEAR Shoemaker* mission. Mineralogical investigation of this family would shed light on the important issues of the source of ordinary chondrites and the rate of orbital diffusion adjacent to a major resonance, and it should allow us to test the proposed main-belt source region for 433 Eros. There is now excellent spectral coverage and mineralogical information for Eros (e.g., *Veverka et al.,* 2000; *Kelley et al.,* 2001a; *McFadden et al.,* 2001; *McCoy et al.,* 2001). To date, however, a rigorous mineralogical assessment of the Maria Family and its potential relationship to Eros has not been done.

5.4. Asteroid Families as Probes of Heliocentric Variations in Asteroid Histories

The variation in asteroid composition with heliocentric distance is some function of the compositional gradient in the solar nebula and the nature and intensity of the early transient heat source. From meteorites, which are naturally delivered samples from a limited set of asteroids, it is well established that an intense heating event took place during the first 2–3 m.y. (~0.05%) of inner solar-system history. Because asteroids suggest a strong heliocentric gradient in this thermal event, there is an implication that it was due to electromagnetic induction heating during a solar T-Tauri episode (e.g., *Herbert et al.,* 1991). The alternate transient heat source, a short-lived radionuclide such as ^{26}Al or ^{60}Fe, would imply either a strong enrichment of these isotopes in the inner nebula or an accretionary wave taking 4–5 m.y. to propagate outward through the inner solar nebula (e.g., *Grimm and McSween,* 1993).

Characterization of the postaccretionary temperatures attained within asteroid parent bodies, derived from their mineralogy and as a function of heliocentric distance, would define the spatial gradient in this early heat source (*Harder-sen and Gaffey,* 2001). For a T-Tauri episode, this thermal gradient constrains the intensity and duration of the presolar outflow and can be used to estimate the total mass lost from the protosolar object. For the short-lived radionuclide option, the thermal gradient would constrain the nebular elemental heterogeneity and/or timing of the planetesimal accretion as a function of heliocentric distance. Based on the concentration of S(IV) asteroids near the 3:1 jovian resonance at 2.5 AU (*Gaffey et al.,* 1993a), the thermal evolution of these asteroids appears to have been retarded by the formation of Jupiter. This should provide a time constraint on the formation of Jupiter once the thermal histories of these asteroids are understood.

Asteroid families provide one of the best means of constraining these thermal and/or compositional gradients. For families passing a genetic test ("true" or "real" families), comparison of the mineralogical compositions of a representative sample of family members allows the degree of internal differentiation to be well defined. This in turn tightly constrains the temperature history and original composition of the specific parent body at the heliocentric location of the family.

6. EXISTING NEEDS, FUTURE DIRECTIONS

There are a number of areas that require further research in order to improve our ability to analyze the reflectance spectra of asteroids. Advances in observational capabilities are now outstripping the interpretive methodologies needed to analyze such data. Some of the more urgent requirements include:

1. Understanding how and to what extent space weathering affects the reflectance spectra of asteroids and our ability to extract diagnostic spectral parameters from such spectra.
2. Developing methods to reliably derive absorption-band areas for mafic silicates in metallic Fe-bearing assemblages.
3. Establishing the optimum wavelength regions and spectral resolutions for detecting the presence and quantifying the abundance and composition of specific minerals.
4. Quantifying the effects of temperature and vacuum on reflectance spectra of various minerals.
5. Defining the effects of very fine-grained and dispersed opaque minerals (e.g., magnetite, troilite) on mafic-silicate reflectance spectra.
6. Expanding the spectral-compositional database for minerals relevant to asteroids, especially low-albedo aster-

oids (e.g., Fe-bearing clays such as those in carbonaceous chondrites, sulfates, etc.).

7. Gaining a more rigorous understanding of the properties that affect the slope and linearity of iron-meteorite spectra.

8. Establishing a quantitative calibration for determining the presence and composition of high Ca-pyroxene in mixtures of olivine, low-Ca pyroxene and high-Ca pyroxene.

Acknowledgments. The authors are grateful for the comments of the editor (A. Cellino) and three reviewers (T. Burbine, R. Binzel, and an anonymous reviewer) whose comments helped to improve this chapter. Support for M.J.G. to carry out this effort came from NASA Planetary Geology and Geophysics Grant NAG5-10345, NASA Exobiology Program Grant NAG5-7598, and NSF Planetary Astronomy Grant AST-9318674. The work of M.S.K. was supported by the NRC Associateships Program. M.J.G., M.S.K., and K.L.R. were visiting astronomers at the Infrared Telescope Facility, operated by the University of Hawai'i under contract to the National Aeronautics and Space Administration.

REFERENCES

Abell P. A. and Gaffey M. J. (2000) Probable geologic composition, thermal history, and meteorite affinities for mainbelt asteroid 349 Dembowska (abstract). In *Lunar and Planetary Science XXXI,* Abstract #1291. Lunar and Planetary Institute, Houston (CD-ROM).

Adams J. B. (1974) Visible and near-infrared diffuse reflectance spectra of pyroxenes as applied to remote sensing of solid objects in the solar system. *J. Geophys. Res., 79,* 4829–4836.

Adams J. B. (1975) Interpretation of visible and near-infrared diffuse reflectance spectra of pyroxenes and other rock-forming minerals. In *Infrared and Raman Spectroscopy of Lunar and Terrestrial Minerals* (C. Karr, ed.), pp. 91–116. Academic, New York.

Adams J. B. and Filice A. L. (1967) Spectral reflectance 0.4 to 2.0 microns of silicate rock powders. *J. Geophys. Res., 72,* 5705–5715.

Adams J. B. and McCord T. B. (1971) Optical properties of mineral separates, glass and anorthositic fragments from Apollo mare samples. *Proc. Lunar Sci. Conf. 2nd,* pp. 2183–2195.

Anders E. (1978) Most stony meteorites come from the asteroid belt. In *Asteroids: An Exploration Assessment* (D. Morrison and W. C. Wells, eds.), pp. 57–78. NASA CP-2053.

Arnold J. R. (1969) Asteroid familes and "jet streams." *Astron. J., 74,* 1235–1242.

Bell J. F. (1989) Mineralogical clues to the origins of asteroid dynamical families. *Icarus, 78,* 426–440.

Binns R. A. (1969) A chondritic inclusion of unique type in the Cumberland Falls meteorite. In *Meteorite Research* (P. Millman, ed.), pp. 696–704. Reidel, Dordrecht.

Binzel R. P. and Xu S. (1993) Chips off of asteroid 4 Vesta: Evidence for the parent body of basaltic achondrite meteorites. *Science, 260,* 186–191.

Binzel R. P., Gaffey M. J., Thomas P. C., Zellner B., Storrs A. D., and Wells E. N. (1997) Geologic mapping of Vesta from 1994 Hubble Space Telescope images. *Icarus, 128,* 95–103.

Bishop J. L. and Pieters C. M. (1995) Low-temperature and low atmospheric pressure infrared reflectance spectroscopy of Mars soil analog materials. *J. Geophys. Res., 100,* 5369–5379.

Bishop J. L., Pieters C. M., and Edwards J. O. (1994) Infrared spectroscopic analysis on the nature of water in montmorillonite. *Clays Clay Minerals, 42,* 702–716.

Bishop J. L., Mustard J. F., Pieters C. M., and Hiroi T. (1998a) Recognition of minor constituents in reflectance spectra of Allan Hills 84001 chips and the importance for remote sensing of Mars. *Meteoritics & Planet. Sci., 33,* 693–698.

Bishop J. L., Pieters C. M., Hiroi T., and Mustard J. F. (1998b) Spectroscopic analysis of Martian meteorite Allan Hills 84001 powder and applications for spectral identification of minerals and other soil components on Mars. *Meteoritics & Planet. Sci., 33,* 699–707.

Brearley A. J. and Jones R. H. (1998) 3. Chondritic meteorites. In *Reviews in Mineralogy, Vol. 36: Planetary Materials* (J. J. Papike, ed.), pp. 3-1 to 3-398. Mineralogical Society of America, Washington, DC.

Britt D. T. and Pieters C. M. (1988) Bidirectional reflectance properties of iron-nickel meteorites. *Proc. Lunar Planet. Sci. Conf. 18th,* pp. 503–512.

Britt D. T. and Pieters C. M. (1991a) Black ordinary chondrites: An analysis of abundance and fall frequency. *Meteoritics, 26,* 279–285.

Britt D. T. and Pieters C. M. (1991b) The bidirectional reflectance spectra of five gas-rich ordinary chondrites (abstract). In *Lunar and Planetary Science XXII,* pp. 139–140. Lunar and Planetary Institute, Houston.

Brouwer D. (1951) Secular variation of the orbital elements of the minor planets. *Astron. J., 56,* 9–32.

Buchanan P. C., Zolensky M. E., and Reid A. M. (1993a) Carbonaceous chondrite clasts in the howardites Bholghati and EET87513. *Meteoritics, 28,* 659–682.

Buchanan P. C., Zolensky M. E., Reid A. M., and Barrett R. A. (1993b) EET87513 clast N: A CM2 fragment in an HED polymict breccia (abstract). In *Lunar and Planetary Science XXIV,* pp. 209–210. Lunar and Planetary Institute, Houston.

Bunch T. E. and Rajan R. S. (1988) Meteorite regolithic breccias. In *Meteorites and the Early Solar System* (J. F. Kerridge and M. S. Matthews, eds.), pp. 144–164. Univ. of Arizona, Tucson.

Burbine T. H., Gaffey M. J., and Bell J. F. (1992) S-asteroids 387 Aquitania and 908 Anacostia: Possible fragments of the breakup of a spinel-bearing parent body with CO3/CV3 affinities. *Meteoritics, 27,* 424–434.

Burbine T. H., Meibom A., and Binzel R. P. (1996) Mantle material in the main belt: Battered to bits? *Meteoritics & Planet. Sci., 31,* 607–620.

Burbine T. H., Buchanan P. C., Binzel R. P., Bus S. J., Hiroi T., Hinrichs J. L., Meibom A., and McCoy T. J. (2000) Vesta, vestoids, and the howardite, eucrite, diogenite group: Relationships and the origin of spectral differences. *Meteoritics & Planet. Sci., 36,* 761–781.

Burns R. G. (1970a) *Mineralogical Applications of Crystal Field Theory.* Cambridge Univ., Cambridge. 224 pp.

Burns R. G. (1970b) Crystal field spectra and evidence of cation ordering in olivine minerals. *Am. Mineral., 55,* 1608–1632.

Burns R. G. (1993) *Mineralogical Applications of Crystal Field Theory,* 2nd edition. Cambridge Univ., Cambridge. 551 pp.

Bus S. J. (1999) Compositional structure in the asteroid belt: Results of a spectroscopic survey. Ph.D. thesis, Massachusetts Institute of Technology, Cambridge. 67 pp.

Bus S. J., Binzel R. P., and Burbine T. H. (1996) Asteroid families: Myth or reality. *Bull. Am. Astron. Soc., 28,* 1097.

Calvin W. M. and King T. V. V. (1997) Spectral characteristics of iron-bearing phyllosilicates: Comparison to Orgueil (CI1), Murchison and Murray (CM2). *Meteoritics & Planet. Sci., 32,* 693–701.

Carvano J. M., Lazzaro D., Mothé-Diniz T., Angeli C. A., and

Florczak M. (2001) Spectroscopic survey of the Hungaria and Phocaea dynamical groups. *Icarus, 149,* 173–189.

Chapman C. R. (1976) Asteroids as meteorite parent-bodies: The astronomical perspective. *Geochim. Cosmochim. Acta, 40,* 701–719.

Chapman C. R. (1987) Distributions of asteroid compositional types with solar distance, body diameter, and family membership. *Meteoritics, 22,* 353–354.

Chapman C. R. (1996) S-type asteroids, ordinary chondrites, and space weathering: The evidence from Galileo's fly-bys of Gaspra and Ida. *Meteoritics & Planet. Sci., 31,* 699–725.

Chapman C. R. and Gaffey M. J. (1979) Reflectance spectra for 277 asteroids. In *Asteroids* (T. Gehrels and M. S. Matthews, eds.), pp. 655–687. Univ. of Arizona, Tucson.

Chapman C. R. and Salisbury J. W. (1973) Comparisons of meteorite and asteroid spectral reflectivities. *Icarus, 19,* 507–522.

Chapman C. R., Paolicchi P., Zappalà V., Binzel R. P., and Bell J. F. (1989) Asteroid families: Physical properties and evolution. In *Asteroids II* (R. P. Binzel et al., eds.), pp. 386–415. Univ. of Arizona, Tucson.

Clark B. E. (1995) Spectral mixing models of S-type asteroids. *J. Geophys. Res., 100,* 14443–14456.

Clark B. E., Hapke B., Pieters C., and Britt D. (2002) Asteroid space weathering and regolith evolution. In *Asteroids III* (W. F. Bottke Jr. et al., eds.), this volume. Univ. of Arizona, Tucson.

Clark R. N. and Lucey P. G. (1984) Spectral properties of ice-particulate mixtures and implications for remote sensing: I. Intimate mixtures. *J. Geophys. Res., 89,* 6341–6348.

Clark R. N., King T. V. V., Klejwa M., Swayze G. A., and Vergo N. (1990) High spectral resolution reflectance spectroscopy of minerals. *J. Geophys. Res., 95,* 12653–12680.

Cloutis E. A. (1996) Spectral properties of hydrocarbon-bearing geological materials (abstract). In *Lunar and Planetary Science XXVII,* pp. 237–238. Lunar and Planetary Institute, Houston.

Cloutis E. A. and Gaffey M. J. (1991a) Pyroxene spectroscopy revisited: Spectral-compositional correlations and relationship to geothermometry. *J. Geophys. Res., 96,* 22809–22826.

Cloutis E. A. and Gaffey M. J. (1991b) Spectral-compositional variations in the constituent minerals of mafic and ultramafic assemblages and remote sensing implications. *Earth Moon Planets, 53,* 11–53.

Cloutis E. A. and Gaffey M. J. (1994) An X-ray diffraction and reflectance spectroscopy study of iron sulphides (abstract). In *Lunar and Planetary Science XXV,* pp. 273–274. Lunar and Planetary Institute, Houston.

Cloutis E. A., Gaffey M. J., Jackowski T. L., and Reed K. L. (1986) Calibration of phase abundance, composition, and particle size distribution for olivine-orthopyroxene mixtures from reflectance spectra. *J. Geophys. Res., 91,* 11641–11653.

Cloutis E. A., Gaffey M. J., Smith D. G. W., and Lambert R. St. J. (1990a) Reflectance spectra of "featureless" materials and the surface mineralogies of M- and E-class asteroids. *J. Geophys. Res., 95,* 281–293.

Cloutis E. A., Gaffey M. J., Smith D. G. W., and Lambert R. St. J. (1990b) Reflectance spectra of mafic silicate-opaque assemblages with applications to meteorite spectra. *Icarus, 84,* 315–333.

Cloutis E. A., Gaffey M. J., Smith D. G. W., and Lambert R. St. J. (1990c) Metal silicate mixtures: Spectral properties and applications to asteroid taxonomy. *J. Geophys. Res., 95,* 8323–8338.

Cruikshank D. P. and Hartmann W. K. (1984) The meteorite-asteroid connection: Two olivine-rich asteroids. *Science, 223,* 281–283.

Deer W. A., Howie R. A., and Zussman J. (1963) *Rock-Forming Minerals, Vol. 2: Chain Silicates.* Longman, London.

Egan W. G., Veverka J., Noland M., and Hilgeman T. (1973) Photometric and polarimetric properties of the Bruderheim chondritic meteorite. *Icarus, 19,* 358–371.

Farinella P., Davis D. R., Cellino A. and Zappalà V. (1992) From asteroid clusters to families: A proposal for a new nomenclature. In *Asteroids, Comets, Meteors 1991* (A. W. Harris and E. Lowell, eds.), pp. 165–166. Lunar and Planetary Institute, Houston.

Farinella P., Gonczi R., Froeschlé Ch., and Froeschlé C. (1993a) The injection of asteroid fragments into resonances. *Icarus, 101,* 174–187.

Farinella P., Froeschlé C., and Gonczi R. (1993b) Meteorites from the asteroid 6 Hebe. *Cel. Mech. Dyn. Astron., 56,* 287–305.

Gaffey M. J. (1976) Spectral reflectance characteristics of the meteorite classes. *J. Geophys. Res., 81,* 905–920.

Gaffey M. J. (1984) Rotational spectral variations of asteroid (8) Flora: Implications for the nature of the S-type asteroids and for the parent bodies of the ordinary chondrites. *Icarus, 60,* 83–114.

Gaffey M. J. (1986) The spectral and physical properties of metal in meteoritic assemblages: Implications for asteroid surface materials. *Icarus, 66,* 468–486.

Gaffey M. J. (1997) Surface lithologic heterogeneity of asteroid 4 Vesta. *Icarus, 127,* 130–157.

Gaffey M. J. (2001) Asteroids: Does space weathering matter? (abstract). In *Lunar and Planetary Science XXXII,* Abstract #1587. Lunar and Planetary Institute, Houston (CD-ROM).

Gaffey M. J. (2002) Asteroid 113 Amalthea: Nature, origin and meteorite affinities of an S(I) assemblage. *Icarus,* submitted.

Gaffey M. J. and Gilbert S. L. (1998) Asteroid 6 Hebe: The probable parent body of the H-type ordinary chondrites and the IIE iron meteorites. *Meteoritics & Planet. Sci., 33,* 1281–1295.

Gaffey M. J., Bell J. F., and Cruikshank D. P. (1989) Reflectance spectroscopy and asteroid surface mineralogy. In *Asteroids II* (R. P. Binzel et al., eds.), pp. 98–127. Univ. of Arizona, Tucson.

Gaffey M. J., Reed K. L., and Kelley M. S. (1992) Relationship of E-type Apollo asteroid 3103 (1982 BB) to the enstatite achondrite meteorites and the Hungaria asteroids. *Icarus, 100,* 95–109.

Gaffey M. J., Bell J. F., Brown R. H., Burbine T. H., Piatek J. L., Reed K. L., and Chaky D. A. (1993a) Mineralogical variations within the S-type asteroid class. *Icarus, 106,* 573–602.

Gaffey M.J., Burbine T. H., and Binzel R. P. (1993b) Asteroid spectroscopy and the meteorite connection: Progress and perspectives. *Meteoritics, 28,* 161–187.

Gaffey M. J., Bell J. F., Brown R. H., Burbine T. H., Piatek J. L., Reed K. L., and Chaky D. A. (1993c) Spectral evidence of size dependent space weathering processes on asteroid surfaces (abstract). In *Lunar and Planetary Science XXIV,* pp. 515–516.

Gaffey S. J., McFadden L. A., Nash D., and Pieters C. M. (1993) Ultraviolet, visible, and near-infrared reflectance spectroscopy: Laboratory spectra of geologic materials. In *Remote Geochemical Analysis: Elemental and Mieralogical Composition* (C. M. Pieters and P. A. J. Englert, eds.), pp. 43–77. Cambridge Univ., Cambridge.

Gomes C. B. and Keil K. (1980) *Brazilian Stone Meteorites.* Univ. of New Mexico, Albuquerque. 162 pp.

Gradie J. and Veverka J. (1986) The wavelength dependence of phase coefficients. *Icarus, 66,* 455–467.

Gradie J. C. and Zellner B. (1977) Asteroid families: Observational evidence for common origins. *Science, 197,* 254–255.

Granahan J. C. (1993) Investigation of asteroid family geology. Ph.D. dissertation, Univ. of Hawai'i, Honolulu. 187 pp.

Grimm R. E. and McSween H. Y. Jr. (1993) Heliocentric zoning of the asteroid belt by aluminum-26 heating. *Science, 259,* 653–655.

Hapke B. (2000) Space weathering in the asteroid belt (abstract). In *Lunar and Planetary Science XXXI*, Abstract #1087. Lunar and Planetary Institute, Houston (CD-ROM).

Hapke B. (2001) Space weathering from Mercury to the asteroid belt. *J. Geophys. Res., 106,* 10039–10073.

Hardersen P. S. and M. J. Gaffey (2001) Unraveling the thermal structure of the asteroid belt from meteoritic and asteroidal evidence (abstract). In *Lunar and Planetary Science XXXII*, Abstract #1103. Lunar and Planetary Institute, Houston (CD-ROM).

Herbert F., Sonett C. P., and Gaffey M. J. (1991) Protoplanetary thermal metamorphism: The protostellar wind electromagnetic induction hypothesis. In *The Sun in Time* (C. P. Sonett et al., eds.), pp. 710–739. Univ. of Arizona, Tucson.

Hirayama K. (1918) Groups of asteroids probably of common origin. *Proc. Phys. Math. Soc. Japan, Ser. 2, No. 9,* 354–361.

Hirayama K. (1933) Present state of the families of asteroids. *Proc. Imp. Acad. Japan, 9,* 482–485.

Hiroi T., Bell J. F., Takeda H., and Pieters C. M. (1993) Modeling of S-type asteroid spectra using primitive achondrites and iron meteorites. *Icarus, 102,* 107–116.

Hiroi T., Binzel R. P., Sunshine J. M., Pieters C. M., and Takeda H. (1995) Grain sizes and mineral compositions of surface regoliths of Vesta-like asteroids. *Icarus, 115,* 374–386.

Howell E. S., Rivkin A. S., Vilas F., and Soderberg A. M. (2001) Aqueous alteration in low albedo asteroids (abstract). In *Lunar and Planetary Science XXXII*, Abstract #2058. Lunar and Planetary Institute, Houston (CD-ROM).

Ingrin J., Latrous K., Doukhan J. C., and Doukhan N. (1989) Water in diopside: An electron microscopy and infrared spectroscopy study. *Eur. J. Mineral., 1,* 327–341.

Jones T. D., Lebofsky L. A., Lewis J. S., and Marley M. S. (1990) The composition and origin of the C, P, and D asteroids: Water as a tracer of thermal evolution in the outer belt. *Icarus, 88,* 172–192.

Keil K. (1982) Composition and origin of chondritic breccias. In *Workshop on Lunar Breccias and Soils and Their Meteoritic Analogs,* pp. 65–83. LPI Tech. Rpt. 82-02, Lunar and Planetary Institute, Houston.

Keil K. (2000) Thermal alteration of asteroids: Evidence from meteorites. *Planet. Space Sci., 48,* 887–903.

Keil K., Bell J. F., and Britt D. T. (1992) Reflection spectra of shocked ordinary chondrites and their relationship to asteroids. *Icarus, 98,* 43–53.

Kelley M. S. and Gaffey M. J. (1996) A genetic study of the Ceres (Williams #67) asteroid family. *Bull. Am. Astron. Soc., 28,* 1097.

Kelley M. S. and Gaffey M. J. (2000) 9 Metis and 113 Amalthea: A genetic asteroid pair. *Icarus, 144,* 27–38.

Kelley M. S. and Gaffey M. J. (2002) High-albedo asteroid 434 Hungaria: Spectrum, composition and genetic connections. *Meteoritics & Planet. Sci.,* in press.

Kelley M. S., Gaffey M. J., and Williams J. G. (1994) Compositional evidence in favor of a genetic link between the Nysa and Hertha asteroid families (abstract). In *Lunar and Planetary Science XXV,* pp. 689–690. Lunar and Planetary Institute, Houston.

Kelley M. S., Gaffey M. J., Vilas F., and Hardersen P. S. (2001a) Recent, ground-based, near-infrared spectral observations of asteroid 433 Eros (abstract). In *Lunar and Planetary Science XXXII*, Abstract #2112. Lunar and Planetary Institute, Houston (CD-ROM).

Kelley M. S., Vilas F., Gaffey M. J., and Abell P. A. (2001b) The first confirmation of a common origin for a small v-class asteroid with 4 Vesta and the HED meteorites. GSA Annual Meeting, Boston, Abstract #20247.

Kelley M. S., Vilas F., Gaffey M. J., and Abell P. A. (2002) Compositional evidence for a common origin of mainbelt asteroid 1929 Kollaa with 4 Vesta and the HED meteorites. *Meteoritics & Planet. Sci.,* in press.

King T. V. V. and Ridley I. W. (1987) Relation of the spectroscopic reflectance of olivine to mineral chemistry and some remote sensing implications. *J. Geophys. Res., 92,* 11457–11469.

Kozai Y. (1979) The dynamical evolution of the Hirayama family. In *Asteroids* (T. Gehrels, ed.), pp. 334–358. Univ. of Arizona, Tucson.

Kring D. A., Hill D. H., Gleason J. D., Britt D. T., Consolmagno G. J., Farmer M., Wilson S., and Haag R. (1999) Portales Valley: A meteorite sample of the brecciated and metal-veined floor of an impact crater on an H-chondrite asteroid. *Meteoritics & Planet. Sci., 34,* 663–669.

Larson H. P., Feierberg M. A., and Lebofsky L. A. (1983) The composition of asteroid 2 Pallas and its relation to primitive meteorites. *Icarus, 56,* 398–408.

Lipschutz M. E., Verkouteren R. M., Sears D. W. G., Hasan F. A., Prinz M., Weisberg M. K., Nehru C. E., Delaney J. S., Grossman L., and Boily M. (1988) Cumberland Falls chondritic inclusions: III. Consortium study of relationship to inclusions in Allan Hills 78113 aubrite. *Geochim. Cosmochim. Acta, 52,* 1835–1848.

Lovering J. F. (1962) The evolution of the meteorites — evidence for the co-existence of chondritic, achondritic and iron meteorites in a typical parent meteorite body. In *Researches on Meteorites* (C. B. Moore, ed.), pp. 179–197. Wiley, New York.

Lucey P. G., Keil K., and Whitely R. (1998) The influence of temperature on the spectra of the A-asteroids and implications for their silicate chemistry. *J. Geophys. Res., 103,* 5865–5871.

Marzari F., Farinella P., and Davis D. R. (1999) Origin, aging, and death of asteroid families. *Icarus, 142,* 63–77.

McCord T. B., Adams J. B., and Johnson T. V. (1970) Asteroid Vesta: Spectral reflectivity and compositional implications. *Science, 168,* 1445–1447.

McCoy T. J., Burbine T. H., McFadden L. A., Starr R. D., Gaffey M. J., Nittler L. R., Evans L. G., Izenberg N., Lucey P. G., Trombka J. I., Bell J. F. III, Clark B. E., Clark P. E., Squyers S. W., Chapman C. R., Boynton W. W., and Veverka J. (2001) The composition of 433 Eros: A mineralogical-chemical synthesis. *Meteoritics & Planet. Sci., 36,* 1661–1672.

McFadden L. A. and Gaffey M. J. (1978) Calibration of quantitative mineral abundances determined from meteorite reflection spectra and applications to solar system objects. *Meteoritics, 13,* 556–557.

McFadden L. A., Wellnitz D. D., Schnaubelt M., Gaffey M. J., Bell J. F. III, Izenberg N., Murchie S., and Chapman C. R. (2001) Mineralogical interpretation of reflectance spectra of Eros from NEAR near-Infrared spectrometer low phase flyby. *Meteoritics & Planet. Sci., 36,* 1711–1726.

McMillan P. F. and Remmele R. L. Jr. (1986) Hydroxyl sites in SiO_2 glass: A note on infrared and Raman spectra. *Am. Mineral., 71,* 772–778.

McSween H. Y. Jr., Bennett M. E. III., and Jarosewich E.(1991) The mineralogy of ordinary chondrites and implications for as-

teroid spectrophotometry. *Icarus, 90,* 107–116.
Merényi E., Howell E. S., Rivkin A. S., and Lebofsky L. A. (1997) Prediction of water in asteroids from spectral data shortward of 3 μm. *Icarus, 129,* 421–439.
Migliorini F., Manara A., Scaltriti F., Farinella P., Cellino A., and Di Martino M. (1997) Surface properties of (6) Hebe: A possible parent body of ordinary chondrites. *Icarus, 128,* 104–113.
Miller G. H., Rossman G. R., and Harlow G. E. (1987) The natural occurrence of hydroxide in olivine. *Phys. Chem. Minerals, 14,* 461–472.
Miyamoto M. (1987) Diffuse reflectance from 0.25 μm to 25 μm of the Yamato-691 enstatite chondrite. *Mem. NIPR Spec. Issue 46,* pp. 123–130. National Institute of Polar Research, Tokyo.
Miyamoto M. (1990) Differences in the degree of weathering between Antarctic and non-Antarctic ordinary chondrites: Infrared spectroscopy. *Workshop on Differences Between Antarctic and Non-Antarctic Meteorites,* pp. 68–71. LPI Tech. Rpt. 90-01, Lunar and Planetary Institute, Houston.
Miyamoto M. (1991) Differences in the degree of weathering between Antarctic and non-Antarctic meteorites inferred from infrared diffuse reflectance spectra. *Geochim. Cosmochim. Acta, 55,* 89–98.
Miyamoto M. and Zolensky M. E. (1994) Infrared diffuse reflectance spectra of carbonaceous chondrites: Amount of hydrous minerals. *Meteoritics, 29,* 849–853.
Miyamoto M., Kojima H., and Yanai K. (1989) Weathering of some Antarctic meteorites: Infrared spectroscopy. *Proc. NIPR Symp. Antarc. Meteorites, 2,* pp. 296–302. National Institute of Polar Research, Tokyo.
Morbidelli A., Gonczi R., Froeschlé Ch., and Farinella P. (1994) Delivery of meteorites through the ν_6 secular resonance. *Astron. Astrophys., 282,* 955–979.
Moroz L. and Arnold G. (1999) Influence of neutral components on relative band contrasts in reflectance spectra of intimate mixtures: Implications for remote sensing.1. Nonlinear mixing modeling. *J. Geophys. Res., 104,* 14109–14121.
Moroz L., Schade U., and Wasch R. (2000) Reflectance spectra of olivine-orthopyroxene-bearing assemblages at decreased temperatures: Implications for remote sensing of asteroids. *Icarus, 147,* 79–93.
Neal C. W. and Lipschutz M. E. (1981) Cumberland Falls chondritic inclusions: Mineralogy/petrology of a forsterite chondrite suite. *Geochim. Cosmochim. Acta, 45,* 2091–2107.
Noble S. K., Pieters C. M., Taylor L. A., Morris R. V., Allen C. C., McKay D. S., and Keller L. P. (2001) The optical properties of the finest fraction of lunar soil: Implications for space weathering. *Meteoritics & Planet. Sci., 36,* 31–42.
Nozette S. and Wilkening L. L. (1982) Evidence for aqueous alteration in a carbonaceous xenolith from the Plainview (H5) chondrite. *Geochim. Cosmochim. Acta, 46,* 557–563.
Ostro S. J., Campbell D. B., and Shapiro I. I. (1985) Mainbelt asteroids: Dual-polarization radar observations. *Science, 229,* 442–446.
Ostro S. J., Campbell D. B., Chandler J. F., Hine A. A., Hudson R. S., Rosema K. D., and Shapiro I. I. (1991) Asteroid 1986 DA: Radar evidence for a metallic composition. *Science, 252,* 1399–1404.
Ostro S. J., Hudson R. S., Nolan M. C., Margot J.-L., Scheeres D. J., Campbell D. B., Magri C., Giorgini J. D., and Yeomans D. K. (2000) Radar observations of asteroid 216 Kleopatra. *Science, 288,* 836–839.
Pellas P. (1991) Exotic clasts in meteoritic breccias (abstract). *Meteoritics, 26,* 384.
Pieters C. M., Fischer E. M., Rode O., and Basu A. (1993) Optical effects of space weathering: The role of the finest fraction. *J. Geophys. Res., 98,* 20817–20824.
Pieters C. M., Taylor L. A., Noble S. K., Keller L. P., Hapke B., Morris R. V., Allen C., McKay D. S., and Wentworth S. (2000) Space weathering on airless bodies: Resolving a mystery with lunar samples. *Meteoritics & Planet. Sci., 35,* 1101–1107.
Pinault L. J., Scott E. D. R, Bogard D. D., and Keil K. (1999) Extraordinary properties of the metal-veined, H6 Portales Valley chondrite: Evidence for internal heating versus shock-melting origins (abstract). In *Lunar and Planetary Science XXX,* Abstract #2048. Lunar and Planetary Institute, Houston (CD-ROM).
Reed K. L., Gaffey M. J., and Lebofsky L. A. (1997) Shape and albedo variations of asteroid 15 Eunomia. *Icarus, 125,* 445–454.
Rivkin A. S., Howell E. S., Britt D. T., Lebofsky L. A., Nolan M. C., and Branston D. D. (1995) 3-μm spectrophotometric survey of M- and E-class asteroids. *Icarus, 117,* 90–100.
Rivkin A. S., Howell E. S., Lebofsky L. A., Clark B. E., and Britt D. T. (2000) The nature of M-class asteroids from 3-μm observations. *Icarus, 145,* 351–368.
Rivkin A. S., Davies J. K., Clark B. E., Trilling D. E., and Brown R. H. (2001) Aqueous alteration on S asteroid 6 Hebe? (abstract). In *Lunar and Planetary Science XXXII,* Abstract #1723. Lunar and Planetary Institute, Houston (CD-ROM).
Rivkin A. S., Howell E. S., Vilas F., and Lebofsky L. A. (2002) Hydrated minerals on asteroids: The astronomical record. In *Asteroids III* (W. F. Bottke Jr. et al., eds.), this volume. Univ. of Arizona, Tucson.
Roedder E., ed. (1984) *Reviews in Mineralogy, Vol. 12: Fluid Inclusions.* Mineralogical Society of America, Washington, DC.
Rubin A. E. and Keil K. (1983) Mineralogy and petrology of the Abee enstatite chondrite breccia and its dark inclusions. *Earth Planet. Sci. Lett., 62,* 118–131.
Rubin A. E. and Ulff-Møller F. (1999) The Portales Valley meteorite breccia: Evidence for impact-induced metamorphism of an ordinary chondrite (abstract). In *Lunar and Planetary Science XXX,* Abstract #1618. Lunar and Planetary Institute, Houston (CD-ROM).
Ruzicka A., Snyder G. A., Prinz M., and Taylor L. A. (1999) Portales Valley: A new metal-phosphate-rich meteorite with affinities to Netschaëvo and H-group chondrites (abstract). In *Lunar and Planetary Science XXX,* Abstract #1645. Lunar and Planetary Institute, Houston (CD-ROM).
Salisbury J. W., Hunt G. R., and Lenhoff C. J. (1975) Visible and near-infrared spectra: X. Stony meteorites. *Mod. Geol., 5,* 115–126.
Salisbury J. W., D'Aria D. M., and Jarosewich E. (1991) Midinfrared (2.5–13.5 μm) reflectance spectra of powdered stony meteorites. *Icarus, 92,* 280–297.
Sandford S. A. (1984) Infrared transmission spectra from 2.5 to 25 μm of various meteorite classes. *Icarus, 60,* 115–126.
Scott E. R. D., Taylor G. J., Newsom H. E., Herbert F., and Zolensky M. (1989) Chemical, thermal and impact processing of asteroids. In *Asteroids II* (R. P. Binzel et al., eds.), pp. 701–739. Univ. of Arizona, Tucson.
Sears D. W., Kallemeyn G. W., and Wasson J. T. (1983) Composition and origin of clasts and inclusions in the Abee enstatite chondrite breccia. *Earth Planet. Sci. Lett., 62,* 180–192.
Singer R. B. and Roush T. L. (1985) Effects of temperature on remotely sensed mineral absorption features. *J. Geophys. Res., 90,* 12434–12444.

Skogby H. and Rossman G. R. (1989) OH^- in pyroxene: An experimental study of incorporation mechanisms and stability. *Am. Mineral., 74,* 1059–1069.

Skogby H., Bell D. R., and Rossman G. R. (1990) Hydroxide in pyroxene: Variations in the natural environment. *Am. Mineral., 75,* 764–774.

Starukhina L. (2001) Water detection on atmosphereless celestial bodies: Alternative explanations of the observations. *J. Geophys. Res., 106,* 14701–14710.

Sunshine J. M., Bus S. J., Burbine T. H., McCoy T. J., and Binzel R. P. (2002) Unambiguous spectral evidence for high- (and low-) calcium pyroxene in asteroids and meteorites (abstract). In *Lunar and Planetary Science XXXIII,* Abstract #1356. Lunar and Planetary Institute, Houston (CD-ROM).

Taylor L. A., Pieters C. M., Keller L. P., Morris R. V., McKay D. S., Patchen A., and Wentworth S. (2001) The effects of space weathering on Apollo 17 mare soils: Petrographic and chemical characterization. *Meteoritics & Planet. Sci., 36,* 285–299.

Tholen D. J. (1984) Asteroid taxonomy from cluster analysis of photometry. Ph.D. thesis, Univ. of Arizona, Tucson. 150 pp.

Tholen D. J. and Barucci M. A. (1989) Asteroid taxonomy. In *Asteroids II* (R. P. Binzel et al., eds.), pp. 298–315. Univ. of Arizona, Tucson.

Trombka J. I., Squyres S. W., Brückner J., Boynton W. V., Reedy R. C., McCoy T. J., Gorenstein P., Evans L. G., Arnold J. R., Starr R. D., Nittler L. R., Murphy M. E., Mikheeva I., McNutt R. L. Jr., McClanahan T. P., McCartney E., Goldsten J. O., Gold R. E., Floyd S. R., Clark P. E., Burbine T. H., Bhangoo J. S., Bailey S. H., and Petaev M. (2000) The elemental composition of asteroid 433 Eros: Results from the NEAR-Shoemaker X-ray spectrometer. *Science, 289,* 2101–2105.

Vaughan D. J. and Craig J. R. (1978) *Mineral Chemistry of Metal Sulfides.* Cambridge Univ., Cambridge.

Verkouteren R. M. and Lipschutz M. E. (1983) Cumberland Falls chondritic inclusions — II. Trace element contents of forsterite chondrites and meteorites of similar redox state. *Geochim. Cosmochim. Acta, 47,* 1625–1633.

Veverka J., Robinson M., Thomas P., Murchie S., Bell J. F. III, Izenberg N., Chapman C., Harch A., Bell M., Carcich B., Cheng A., Clark B., Domingue D., Dunham D., Farquhar R., Gaffey M. J., Hawkins E., Joseph J., Kirk R., Li H., Lucey P., Malin M., Martin P., McFadden L., Merline M. J., Miller J. K., Owen W. M. Jr., Peterson C., Prockter L., Warren J., Wellnitz D., Williams B. G., and Yeomans D. K. (2000) NEAR at Eros: Imaging and spectral results. *Science, 289,* 2088–2097.

Vilas F. and Gaffey M. J. (1989) Identification of phyllosilicate absorption features in main-belt and outer-belt asteroid reflectance spectra. *Science, 246,* 790–792.

Vilas F. and McFadden L. A. (1992) CCD reflectance spectra of selected asteroids. I. Presentation and data analysis considerations. *Icarus, 100,* 85–94.

Vilas F. and Smith B. A. (1985) Reflectance spectrophotometry (0.5–1.0 μm) of outer-belt asteroids: Implications for primitive, organic solar system material. *Icarus, 64,* 503–516.

Vilas F., Hatch E. C., Larson S. M., Sawyer S. R., and Gaffey M. J. (1993) Ferric iron in primitive asteroids: A 0.43-μm absorption feature. *Icarus, 102,* 225–231.

Vilas F., Jarvis K. S., and Gaffey M. J. (1994) Iron alteration minerals in the visible and near-infrared spectra of low-albedo asteroids. *Icarus, 109,* 274–283.

Vilas F., Cochran A. L., and Jarvis K. S. (2000) Vesta and the Vestoids: A new rock group? *Icarus, 147,* 119–128.

Wagner C., Arnold G., and Wäsch R. (1988) The infrared transmission spectrum of the Salzwedel meteorite. *Meteoritics, 23,* 93–94.

Walker D. and Grove T. (1993) Ureilite smelting. *Meteoritics, 28,* 629–636.

Watson F. G. (1941) *Between the Planets*. Harvard Books on Astronomy, Blakiston, Philadelphia. 222 pp.

Wetherill G. W. and Chapman C. R. (1988) Asteroids and meteorites. In *Meteorites and the Early Solar System* (J. F. Kerridge and M. S. Matthews, eds), pp. 35–67. Univ. of Arizona, Tucson.

Wilkening L. L. (1977) Meteorites in meteorites: Evidence for mixing among the asteroids. In *Comets, Asteroids, Meteorites: Interrelations, Evolution and Origins* (A. H. Delsemme, ed.), pp. 389–396. Univ. of Toledo, Toledo.

Williams J. G. (1989) Asteroid family identifications and proper elements. In *Asteroids II* (R. P. Binzel et al., eds.), pp. 1034–1072. Univ. of Arizona, Tucson.

Williams J. G. (1992) Asteroid families — An initial search. *Icarus, 96,* 251–280.

Xu S., Binzel R. P., Burbine T. H., and Bus S. J. (1995) Small main-belt asteroid spectroscopic survey: Initial results. *Icarus, 115,* 1–35.

Yanai K., Matsumoto Y., and Kojima H. (1983) A Brachina-like inclusion in the Yamato-75097 L6 chondrite: A preliminary examination. *Proc. 8th Symp. Antarc. Meteorites, NIPR Spec. Issue 30,* pp. 29–35. National Institute of Polar Research, Tokyo.

Zappalà V., Cellino A., Farinella P., and Knežević Z. (1990) Asteroid families. I. Identification by hierarchical clustering and reliability assessment. *Astron. J., 100,* 2030–2046.

Zappalà V., Cellino A., Farinella P., and Milani A. (1994) Asteroid families: II. Extension to unnumbered and multiopposition asteroids. *Astron. J., 107,* 772–801.

Zappalà V., Bendjoya Ph., Cellino A. , Farinella P., and Froeschlé C. (1995) Asteroid families: Search of a 12,487-asteroid sample using two different clustering techniques. *Icarus, 116,* 291–314.

Zappalà V., Cellino A., Di Martino M., Migliorini F., and Paolicchi P. (1997) Maria's family: Physical structure and possible implications for the origin of giant NEAs. *Icarus, 129,* 1–20.

Zellner B. (1975) 44 Nysa: An iron-depleted asteroid. *Astrophys. J. Lett., 198,* L45–L47.

Zolensky M. E., Barrett R. A., and Ivanov A. V. (1991) Mineralogy and matrix composition of CI clasts in the chondritic breccia Kaidun (abstract). In *Lunar and Planetary Science XXII,* pp. 1565–1566. Lunar and Planetary Institute, Houston.

Zolensky M. E., Weisberg M. K., Barrett R. A., and Prinz M. (1993) Mineralogy of dark clasts in primitive versus differentiated meteorites (abstract). In *Lunar and Planetary Science XXIV,* pp. 1583–1584. Lunar and Planetary Institute, Houston.

Zolensky M. E., Bodnar R. J., Gibson E. K. Jr., Nyquist L. E., Reese Y., Shih C.-Y., and Wiesmann H. (1999a) Asteroidal water within fluid inclusion-bearing halite in an H5 chondrite, Monahans (1998). *Science, 285,* 1377–1379.

Zolensky M. E., Bodnar R. J., and Rubin A. E. (1999b) Asteroidal water within fluid inclusion-bearing halite in ordinary chondrites (abstract). *Meteoritics & Planet. Sci., 34,* A124.